acid-independent human rotavirus strain. J Virol. 2006;80:1513-1523.
39. Komoto, S., Sasaki, J., Taniguchi, K.: Reverse genetics system for introduction of site-specific mutations into the double-stranded RNA genome of infectious rotavirus. Proc. Natl. Acad. Sci. USA (in press)
40. Okada M et al.: Genetic analysis of noroviruses in Chiba Prefecture, Japan, between 1999 and 2004. J. Clin. Microbiol. 2005;43:4391-4401
41. Seto Y, Iritani N, Kubo H, Kaida A, Murakami T, Haruki K, Nishio O, Ayata M, and Ogura T: Genotyping of norovirus strains detected in outbreaks between April 2002 and March 2003 in Osaka City, Japan, Microbiol. Immunol. 2005;49:275-283.
42. Hirakata Y, Arisawa K, Nishio O, Nakagomi O. Multifectural spread of gastroenteritis outbreaks attributable to a single genogroup II norovirus strain from a tourist restaurant in Nagasaki, Japan. J. Clin. Microbiol. 2005;43:1093-1098.
43. Phan TG, Okame M, Nguyen TA, Nishio O, Okitsu S, Ushijima H. Genetic of Sapovirus in fecal specimens from infants and children with acute gastroenteritis in Pakistan. Arch Virol. 2005;150:371-377.
44. Oka T., Katayama K., Ogawa S., Hansman GS., Kageyama T., Ushijima H., Miyamura T., and Takeda N.. Proteolytic Processing of Sapovirus ORF1 Polyprotein. J. Virol. 2005; 79:7283-90.
45. Hansman GS., Matsubara N., Oka T., Ogawa S., Natori K., Takeda N., and Katayama K. Deletion analysis of the Sapovirus VP1 gene for the assembly of virus-like particles. Archives of Virology. 2005;150:2529-2538.
46. Oka T., Katayama K., Ogawa S., Hansman GS., Kageyama T., Miyamura T., and Naokazu Takeda. Cleavage activity of the Sapovirus 3C-like protease in *Escherichia coli*. Arch. Virol. 2005;150:2539-2548.
47. Hansman GS., Takeda N., Oka T., Oseto M., Hedlund KO., and Katayama K. Intergenogroup recombination in sapoviruses. Emerg. Infect. Dis. 2005;11:1916-1920.
48. Oka T., Hansman GS., Katayama K., Ogawa S., Nagata N., Miyamura T., Takeda N. Expression of sapovirus virus-like particles in mammalian cells. Arch. Virol. 2006;151:399-404.
49. Wu FT., Oka T., Katayama K., Wu HS., Donald Jiang DS., Miyamura T., Takeda N., and Hansman GS. Genetic diversity of noroviruses in Taiwan between November 2004 and March 2005. Arch. Virol. In press
50. Hansman GS., Natori K., Shirato-Horikoshi H., Ogawa S., Oka T., Katayama K., Tanaka T., Miyoshi T., Sakae K., Kobayashi S., Shinohara M., Uchida K., Sakurai N., Shinozaki K., Okada M., Seto Y., Kamata K., Miyamura T. and Takeda N. Genetic and antigenic diversity among noroviruses. J. Gen. Virol. In press
51. Katayama K., Hansman GS., Oka T., Ogawa S., Takeda N. Investigation of Norovirus replication in a human cell line. Arch. Virol. In press
52. 田中智之 「微生物の基礎知識」ノロウイルス 感染と消毒 2004;11;28-31

53. 斎藤博之、ノロウイルスによる胃腸炎の流行形態と対策、クリーンネス 231:2-7、2005
54. 杉枝正明、新川奈緒美、大瀬戸光明、徳竹由美、山口卓、秋山美穂、西尾治: Norovirus 感染により排泄されるウイルス量について、臨床とウイルス 32:189-194、2004
55. 新川奈緒美、川元孝久、秋山美穂、加藤由美子、西尾治：吐物が感染源と推察されたノロウイルス集団胃腸炎事例について、臨床とウイルス 32:195-201、2004
56. 西尾治、秋山美穂、愛木智香子：ノロウイルスによる食中毒、月刊 HACCP、109：48-50、2004
57. 白土（堀越）東子、武田直和：冬でも怖い食中毒（冬の食生活予防は万全ですか？）． 食生活：98 2004.
58. 武田直和、米山徹夫、清水博之、白土（堀越）東子：食品由来の感染症． ネオエカス 感染症・アレルギーと生体防御 11-20, 2005.
59. 白土(堀越)東子:ノロウイルスによる感染性胃腸炎の集団発生． 生活と環境 2005;50:8-13.
60. 椛島由佳, 伊藤 雅, 山下照夫, 藤浦 明, 榮 賢司: 臨床とウイルス. 33:228-233, 2005
61. 山下育孝、近藤玲子、豊嶋千俊、大瀬戸光明、井上博雄、愛木智香子、秋山美穂、西尾 治. 散発性胃腸炎と胃腸炎集団発生からのノロウイルス検出状況－愛媛県、病原微生物検出情報, 26：327-329, 2005
62. 山下育孝、近藤玲子、豊嶋千俊、大瀬戸光明、井上博雄、杉枝正明、古屋由美子、愛木智香子、秋山美穂、西尾 治. 輸入生鮮魚介類からのノロウイルス検出状況とその遺伝子型、病原微生物検出情報 26：337-338, 2005
63. 斎藤博之 他、簡易水道が原因と考えられたノロウイルスの流行、病原微生物検出情報 26:14-15 (2005)
64. 斎藤博之 他、エンテロウイルスの血清型別同定における一本鎖高次構造多型（SSCP）解析の応用、臨床とウイルス 33:220-227 (2005)
65. 斎藤博之、ノロウイルス胃腸炎の疫学調査における一本鎖高次構造多型(SSCP)解析の利用、食中毒検査と診療の落とし穴、第 2 章、中山書店 (2006)
66. 斎藤博之、ノロウイルス胃腸炎の流行拡大防止、食中毒検査と診療の落とし穴、第 5 章、中山書店 (2006)
67. 久保英幸, 改田 厚, 入谷展弘, 村上 司：2000-2002 年に世界的流行の認められたエコーウイルス 13 型の大阪市での分離株を含む遺伝子系統樹解析. 生活衛生 49:144-151 (2005)
68. 入谷展弘, 勢戸祥介, 春木孝祐, 西尾 治, 久保英幸, 改田 厚, 村上 司, 綾田 稔, 小倉壽：市販生カキからのノロウイルスおよび A 型肝炎ウイルスの検出. 生活衛生 49:279-287 (2005)
69. 西尾治, 古屋由美子, 大瀬戸光明. ウイルス性食中毒の予防―ノロウイルス, A 型肝炎ウイルス―. 食品衛生研究 55:19-24, 2005.
70. 西尾治. ノロウイルスの感染と遺伝子迅速検査の現状と期待. The Medical Journal. 915:11, 2005.
71. 西尾治. ノロウイルスによる感染症と食中毒. 日本医事新報 4221:105, 2005.
72. 西田知子, 岡本玲子, 中尾利器, 松村健道, 大瀬戸光明, 西尾治. 山口県内におけるノロウイルス胃腸炎集団発生事例および市販生食カキの汚染状況. 獣医公衆衛生研究 7:24-25, 2005.

73. 西尾治. 広範囲 血液･尿化学検査免疫学的検査―その数値をどう読むか―ノロウイルス. 日本臨床 63巻増刊号7:332-333, 2005.
74. 西尾治, 山下育孝, 宇宿秀三. ノロウイルスによる食中毒, 感染症. 食品衛生研究 55:7-16, 2005.
75. 西尾治, 秋山美穂, 愛木智香子, 杉枝正明, 福田伸治, 西田知子, 植木洋, 入谷展弘, 篠原美千代, 木村博一. ノロウイルスによる食中毒について. 食品衛生学雑誌 46:235-245, 2005.
76. 白土（堀越）東子、岡 智一郎、片山和彦、武田直和：ノロウイルス研究の最近の動向. 感染・炎症・免疫 35: 106-117, 2005.
77. 白土（堀越）東子：誰もが感染の危機！！ノロウイルス. 食と健康 49(11): 53-57, 2005.
78. 米山徹夫、李天成、白土（堀越）東子、武田直和：食品産業従事者のためのウイルス基礎知識. ジャパンフードサイエンス 印刷中

JOURNAL OF VIROLOGY, Apr. 2004, p. 3817–3826 Vol. 78, No. 8
0022-538X/04/$08.00+0 DOI: 10.1128/JVI.78.8.3817–3826.2004

Genogroup II Noroviruses Efficiently Bind to Heparan Sulfate Proteoglycan Associated with the Cellular Membrane

Masaru Tamura,[1,2]† Katsuro Natori,[1] Masahiko Kobayashi,[2] Tatsuo Miyamura,[1] and Naokazu Takeda[1]*

Department of Virology II, National Institute of Infectious Diseases, Musashi-Murayama, Tokyo 208-0011,[1] and Graduate School of Agricultural and Life Sciences, The University of Tokyo, Bunkyo-ku, Tokyo 113-8657,[2] Japan

Received 15 August 2003/Accepted 12 December 2003

Norovirus **(NV), a member of the family *Caliciviridae*, is one of the important causative agents of acute gastroenteritis. In the present study, we found that virus-like particles (VLPs) derived from genogroup II (GII) NV were bound to cell surface heparan sulfate proteoglycan. Interestingly, the VLPs derived from GII were more than ten times likelier to bind to cells than were those derived from genogroup I (GI). Heparin, a sulfated glycosaminoglycan, and suramin, a highly sulfated derivative of urea, efficiently blocked VLP binding to mammalian cell surfaces. The reagents known to bind to cell surface heparan sulfate, as well as the enzymes that specifically digest heparan sulfate, markedly reduced VLP binding to the cells. Treatment of the cells with chlorate revealed that sulfation of heparan sulfate plays an important role in the NV-heparan sulfate interaction. The binding efficiency of NV to undifferentiated Caco-2 (U-Caco-2) cells differed largely between GI NV and GII NV, whereas the efficiency of binding to differentiated Caco-2 (D-Caco-2) cells did not differ significantly between the two genogroups, although slight differences between strains were observed. Digestion with heparinase I resulted in a reduction of up to 90% in U-Caco-2 cells and a reduction of up to only 50% in D-Caco-2 cells, indicating that heparan sulfate is the major binding molecule for U-Caco-2 cells, while it contributed to only half of the binding in the case of D-Caco-2 cells. The other half of those VLPs was likely to be associated with H-type blood antigen, suggesting that GII NV has two separate binding sites. The present study is the first to address the possible role of cell surface glycosaminoglycans in the binding of recombinant VLPs of NV.**

Norovirus (NV), a member of the family *Caliciviridae*, is a causative agent of acute gastroenteritis, and NV is known to have been responsible for both sporadic cases and epidemic outbreaks of the disease in both developing and developed countries (23, 55). As many as 95% of nonbacterial gastroenteritis outbreaks in the world are reported to be caused by this agent (20). Most of the outbreaks are associated with the ingestion of contaminated food, in particular raw shellfish, or contaminated drinking water (24, 39, 55). The predominant clinical manifestations are nausea, vomiting, and diarrhea (38). In 1972, 27-nm-diameter viral particles of the prototype NV strain (Hu/NV/GI/Norwalk/1968/US, NV/68) were identified by immune electron microscopy in fecal specimens collected from a patient during a gastroenteritis outbreak at an elementary school in Norwalk, Ohio, in the year 1968 (1, 37).

NV is a nonenveloped virus containing an approximately 7.5-kb, positive-sense, single-stranded RNA genome with a polyadenylated tail at the 3′ end (33). The genome contains three open reading frames (ORFs), with ORF1 encoding nonstructural proteins and ORF2 and ORF3 encoding structural proteins (18). Currently, NV is classified into two genogroups, genogroup I (GI) and GII, according to the nucleotide and amino acid sequences (4, 21, 40).

In spite of extensive efforts, biochemical studies of NV have been hampered by the lack of a cell culture system in which the virus will grow, although one animal model has recently been reported (67). Only chimpanzees developed serologic responses when inoculated with NV/68, but they usually underwent an asymptomatic infection (82). Most of our understanding of NV infection has been obtained from epidemiological and volunteer studies (25, 52, 57, 64).

Recombinant baculoviruses harboring the gene encoding the NV capsid protein have been constructed, and the proteins were expressed in insect cells (34). An approximately 58-kDa capsid protein appeared to be self-assembled into virus-like particles (VLPs). The fine structure of the recombinant VLPs of NV/68 (rNV/68) was elucidated by electron cryomicroscopy and X-ray crystallography, and it was found that rNV/68 is composed of 180 capsid proteins that form an icosahedron that is 38 nm in diameter (59, 60). Green and coworkers determined that rNV/68 is morphologically and antigenically similar to the native virions (22). Hyperimmune sera against rNV/68 were subsequently prepared, and enzyme-linked immunosorbent assays were established for the detection of NV/68 in stool specimens (19). It was also found that rNV/68 was immunogenic, and rNV/68 has been used for oral immunization to evaluate its ability to stimulate mucosal immunity (6, 26, 50). VLPs have also been useful for studying virus-cell interactions in vitro (7, 58, 80).

* Corresponding author. Mailing address: Department of Virology II, National Institute of Infectious Diseases, 4-7-1 Gakuen, Musashi-Murayama, Tokyo 208-0011, Japan. Phone: 81-42-561-0771. Fax: 81-42-561-4729. E-mail: ntakeda@nih.go.jp.

† Present address: Department of Genetics, Stanford University School of Medicine, Stanford, CA 94305.

It remains unclear where NV infects the host and subsequently multiplies, although the jejunum from volunteers with NV infection exhibited histopathological lesions (63, 64). Knowledge of the molecular basis for the interaction between NV and target cells may facilitate the development of vaccines and provide pharmaceutical strategies for the prevention and treatment of NV infection. In a previous study, we prepared VLPs from Ueno virus (UEV), a GII NV, and found a 105-kDa protein as a candidate receptor molecule (71). However, attempts to extract and purify the 105-kDa protein have remained unsuccessful. Recently, the association between NV infection and histo-blood group antigens present on host secretor intestinal cells has been reported (28, 31, 46, 49), and hemagglutination by rNV/68 was observed (32).

In the present study, we compared the binding of VLPs from both GI NV and GII NV to intestinal cells and found that the binding of GII NV VLPs to the cells occurred more efficiently than those of GI NV. We used ileum Intestine 407 cells, from human small intestine, to investigate the cell surface binding molecules. Assays using various inhibitors and enzymatic modifications of the cell surface revealed that NV binding was mediated by heparan sulfate proteoglycan, and this interaction was ubiquitously observed in various cell lines.

MATERIALS AND METHODS

Cells. Intestine 407 (human ileum) cells were grown at 37°C with Dulbecco's modified Eagle's medium (D-MEM) (Sigma Chemical Co., St. Louis, Mo.) containing recombinant human insulin (10 μg/ml; Wako Pure Chemical Industries, Ltd., Osaka, Japan) and 10% fetal bovine serum (FBS) (JRH Biosciences, Lenexa, Kans.). CHO (Chinese hamster ovary) cells, HeLa (human cervix) cells, Vero (African green monkey kidney) cells, and A549 (human alveolar type II-derived carcinoma) cells were grown at 37°C with D-MEM containing 10% FBS. Tn5 cells, derived from the insect *Trichoplusia ni* (30), were grown at 27°C with Ex-CELL 400 (JRH Biosciences). Caco-2 (human colon) cells were grown at 37°C with GIT medium (Wako) containing 3% FBS. Caco-2 cells are known to spontaneously differentiate into enterocyte-like cells more than 6 days postconfluency. The cells showed biochemical and morphological features of differentiation, such as sucrase activity and the presence of domes (2, 80). The cells were incubated for at least 10 days posteonfluency and were used as differentiated Caco-2 (D-Caco-2) cells, which represented typical domes.

Recombinant VLPs. Two strains from GI NV (Seto 124 virus [SEV] [43] and Funabashi virus [FUV] [AB078335] [unpublished data]) and three strains from GII NV (Ueno 7k virus [UEV] [AB078337] [71], Chitta 76 virus [CHV] [42], and Kashiwa 47 virus [KAV] [AB078334] [unpublished data]) were used. ^{35}S-labeled or nonlabeled VLPs were prepared by utilizing baculovirus expression systems with Tn5 insect cells, as described previously (71). Briefly, Tn5 cells in a 250-ml flask were infected with a recombinant baculovirus harboring NV ORF2 at a multiplicity of infection of 5 to 10, and the cells were incubated for 24 h at 27°C. The NV capsid proteins were metabolically radiolabeled with L-[^{35}S]methionine (Tran^{35}S-Label metabolic labeling reagent [30 μCi/ml]; ICN Biomedicals, Inc.) for 12 h at 27°C. Seven days after infection, the cells were harvested and the ^{35}S-labeled rNV were purified by CsCl equilibrium density gradient centrifugation followed by 5-to-30% sucrose gradient centrifugation. The specific activities of the purified ^{35}S-labeled-rSEV, -rFUV -rUEV, -rCHV, and -rKAV were 2.2×10^4, 1.2×10^4, 9.6×10^3, 5.9×10^3, and 2.7×10^3 cpm/μg, respectively.

Inhibitory agents and enzyme digestion. Heparin sodium salt, suramin sodium salt, protamine sulfate grade X (from salmon), poly-L-lysine hydrobromide (molecular weight, 30,000 to 70,000), magainin I, and cecropin A were obtained from Sigma Chemical Corporation. Glycosaminoglycans, heparan sulfate sodium salt (from bovine kidney), chondroitin sulfate C sodium salt (from shark cartilage), and hyaluronic acid (from bovine vitreous humor) were obtained from Sigma Chemical Co. Dermatan sulfate I (from porcine intestinal mucosa) was obtained from ICN Pharmaceuticals, Inc. (Costa Mesa, Calif.). Blood group H disaccharide, blood group A trisaccharide, and blood group B trisaccharide were obtained from Calbiochem-Novabiochem Co. (La Jolla, Calif.). Those chemicals were dissolved in either distilled water or phosphate-buffered saline (pH 7.5; Nissui Pharmaceutical Co. Ltd., Tokyo, Japan).

Heparinase I, heparinase III (heparitinase), and chondroitinase ABC (from *Proteus vulgaris*) were obtained from Sigma Chemical Co. α1,2-Fucosidase (from *Xanthomonas* sp.) was obtained from Calbiochem-Novabiochem Co. They were dissolved in serum-free D-MEM. Enzyme digestion was carried out in serum-free D-MEM at 37°C for 60 min. Under the present assay conditions, none of these enzymatic treatments caused any detachment of cells from the monolayers.

Binding assay. Confluent monolayers of various mammalian cells in a 24-well collagen-coated plate (Asahi Techno Glass Co. Ltd., Tokyo, Japan) (10^5 to 10^6 cells/well) were incubated with 15 μg of ^{35}S-labeled VLPs in either the presence or absence of inhibitors for 1 h at 4°C. All reactions were performed in a final volume of 200 μl of serum-free D-MEM. Free ^{35}S-labeled-VLPs were eliminated by washing the cells three times with serum-free D-MEM, and the cells were solubilized with radioimmunoprecipitation assay (RIPA) buffer (0.15 M NaCl, 1% sodium deoxycholate, 1% Triton X-100, 0.1% sodium dodecyl sulfate, 0.01% aprotinin, 10 mM Tris-HCl [pH 7.2]). The radioactivity was then measured with a liquid scintillation counter. Assays were performed in triplicate.

Inhibition of glycosaminoglycan sulfation. Low-sulfate medium D-MEM/F-12 was obtained from GIBCO BRL (Gaithersburg, Md.) and supplemented with 10% FBS. Vero cells were cultured in D-MEM or low-sulfate D-MEM/F-12 for 48 h in 24-well plates in the presence of the sulfation inhibitor sodium chlorate (5). Replicate cells were supplemented with sodium sulfate in order to assess the sulfation-specificity of inhibition.

RESULTS

The binding of VLPs of GI NV and GII NV to cells. NV is classified into two genogroups, GI and GII, according to the nucleotide and amino acid sequences (45, 78). Each genogroup contains many genetic clusters forming the various genotypes. We used a virus-binding assay to compare the NV binding efficiency between the two genogroups, as described previously (71). ^{35}S-labeled VLPs were prepared from five NV strains, and we compared the binding efficiency to Intestine 407 cells, a cell line derived from human intestine, and CHO cells, a cell line derived from Chinese hamster ovary. The binding of three recombinant VLPs of GII NV (rUEV, rKAV, and rCHV) to Intestine 407 cells appeared to be more efficient than those of either of the two VLPs of GI NV (rSEV and rFUV) (Fig. 1A). Similar results were obtained when CHO cells were used. The binding of rUEV to CHO cells was also more efficient than that of rSEV and rFUV, indicating that VLPs of GII NV were able to bind more efficiently to these cells than did the VLPs of GI NV (Fig. 1B).

The binding of rUEV to Intestine 407 cells via negatively charged cell surface molecule(s). To account for the discrepancies between the binding efficiencies observed between GI NV and GII NV, we investigated cell surface molecule(s) involved in the binding process. We used six potential binding inhibitors to study the binding of rUEV to Intestine 407 cells (Fig. 2). Heparin and suramin were known to bind to polycations on the surfaces of various virus particles and cell surface molecules (11, 53, 75). Poly-L-lysine and protamine sulfate, heparin antagonists, are known to bind to polyanions. Magainin I, a positively charged peptide (85), and cecropin A (66) are antimicrobial and antiviral peptides.

As depicted in Fig. 2A, when the assay was performed in the presence of heparin, the binding of rUEV to Intestine 407 cells was decreased in a dose-dependent manner. However, this inhibition of binding was not observed when the cells were pretreated with heparin (2.5 μg/ml), indicating that heparin blocks the binding of rUEV to cells by associating with rUEV, and not with the cells. Similar results were observed when suramin was used (Fig. 2B). Poly-L-lysine and protamine sulfate similarly inhibited the binding of rUEV in a dose-depen-

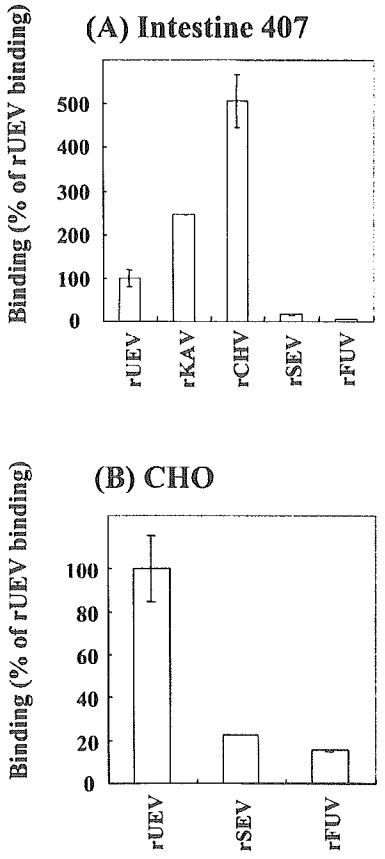

FIG. 1. Comparison of binding efficiency. Fifteen micrograms of ^{35}S-labeled VLPs from GI (rSEV and rFUV) and GII (rUEV, rKAV, and rCHV) was incubated for 1 h at 4°C with the cells placed in 24-well plates. The cells were washed, and the radioactivity was measured. The results are expressed as the percentage of ^{35}S-labeled rUEV binding. The mean values were plotted (error bars, standard deviation ranges). The experiments were performed in triplicate and were reproduced at least twice. (A) Intestine 407 cells were incubated with ^{35}S-labeled rUEV, rKAV, rCHV, rSEV, and rFUV. (B) CHO cells were incubated with ^{35}S-labeled rUEV, rSEV, and rFUV.

dent manner (Fig. 2C and D). However, strong inhibition was also observed when the cells were treated before being exposed to rUEV, demonstrating that these two reagents caused an inhibitory effect by directly binding to the cells. This observation was in contrast to that of heparin and suramin. Cecropin A, magainin I, and bovine serum albumin (BSA) had no effect on the binding of rUEV (Fig. 2E and F).

Although heparin is not a constituent of cell membranes, this molecule is a structural homologue of heparan sulfate, a negatively charged glycosaminoglycan (56). Heparan sulfate is widely expressed on the cell surface and in extracellular matrices (29, 36). Poly-L-lysine and protamine sulfate are known to bind to cell surface polyanions. Therefore, negatively charged Intestine 407 cell surface molecules, such as sulfated glycosaminoglycans, are likely to be involved in the binding of rUEV.

rUEV interacts with negatively charged glycosaminoglycans. To determine whether a negatively charged cell surface glycosaminoglycan is associated with binding to the cell surface, we selected four major soluble glycosaminoglycans (i.e., heparan sulfate, chondroitin sulfate C, dermatan sulfate I [chondroitin sulfate B], and hyaluronic acid) as competitive antagonists. As depicted in Fig. 3, heparan sulfate, chondroitin sulfate C, and dermatan sulfate I showed dose-dependent inhibition, which was distinguished at doses of 50 μg/ml and higher (Fig. 3A to C). These three glycosaminoglycans have a negatively charged sulfate group (27). No inhibition was observed when the cells were pretreated with any one of these compounds at a concentration of 50 μg/ml, indicating that they all successfully block binding by associating with rUEV, and not with Intestine 407 cells. In contrast, hyaluronic acid, which has no charged group in the molecule, had no effect, even when concentrations up to 200 μg/ml were tested (Fig. 3D). These results indicated that negatively charged glycosaminoglycans are capable of easily binding to rUEV and that they inhibit the binding of rUEV to Intestine 407 cells. The findings therefore suggest that glycosaminoglycans on the cell surface play a role in the binding of rUEV to the cell surface.

The cell surface molecule involved in binding is heparan sulfate glycosaminoglycan. To determine whether or not cell surface glycosaminoglycan is actually used in the binding process, we pretreated Intestine 407 cells with glycosaminoglycan-specific lyases and measured the extent of ^{35}S-labeled rUEV binding. The cells were exposed to three different enzymes capable of digesting cell surface glycosaminoglycan moieties, namely, heparinase I, heparinase III, and chondroitinase ABC. Heparinase I cleaves glycosidic linkages in both heparin and heparan sulfates, while heparinase III selectivity cleaves the linkages in heparan sulfate (47, 56). Chondroitinase ABC specifically cleaves glycosidic linkages in chondroitin sulfates A, B, and C (83), which are also major glycosaminoglycans on cell surfaces.

Digestion with either heparinase I or heparinase III resulted in a marked reduction of the binding of ^{35}S-labeled rUEV in a dose-dependent manner (Fig. 4A and B), while digestion with chondroitinase ABC had no influence on the binding (Fig. 4C). We also confirmed that digestion with heparinase I (10 U/ml) resulted in a reduction of more than 90% of the ^{35}S-labeled rCHV binding to Intestine 407 cells (data not shown). These results indicated that cell surface heparan sulfate glycosaminoglycan is the major molecule involved in the binding, at least as regards these two strains of GII NV.

Sulfation of glycosaminoglycans is required for binding. Hyaluronic acid was not associated with an inhibitory effect on cell surface binding (Fig. 3D), and this molecule is the only nonsulfated glycosaminoglycan among the potent inhibitors (27). This result suggested that the sulfation of glycosaminoglycan is important for rUEV binding to cells. To further clarify this point, we cultivated Vero cells in low-sulfate medium D-MEM/F-12 with a specific sulfation inhibitor, sodium chlorate (5), and measured the binding of ^{35}S-labeled rUEV to the cells. The addition of sodium chlorate led to a marked dose-dependent loss of binding (Fig. 5). The lack of rUEV binding due to desulfation by sodium chlorate was recovered dose dependently by supplementing the cells with sodium sulfate (Fig. 5). These results thus demonstrated that sulfation of glycosaminoglycan plays an important role in the binding of rUEV.

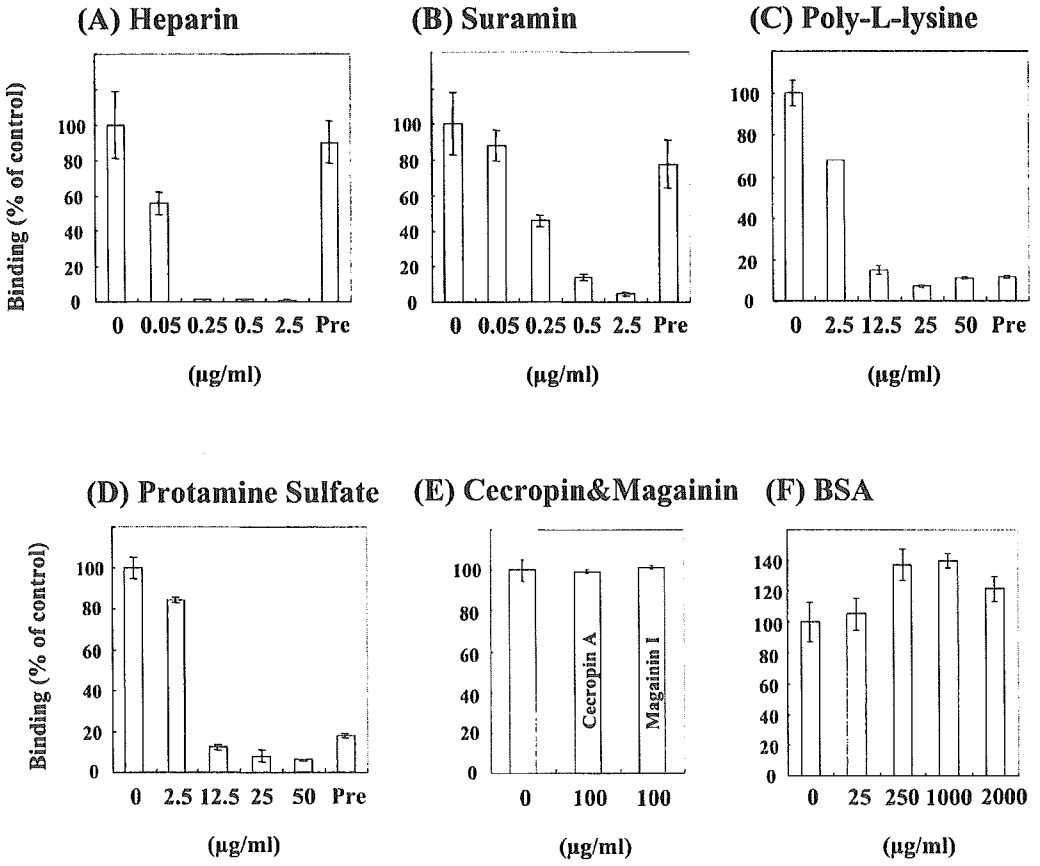

FIG. 2. Inhibition of binding with various inhibitory molecules. Intestine 407 cell monolayers were incubated with ^{35}S-labeled rUEV in the presence of increasing concentrations of potential inhibitors: heparin (A), suramin (B), poly-L-lysine (C), protamine sulfate (D), cecropin A (100 μg/ml) and magainin I (100 μg/ml) (E), and BSA (F). The cells were also preincubated with each compound at concentrations of 2.5 μg/ml (heparin and suramin) and 50 μg/ml (poly-L-lysine and protamine sulfate), washed three times, incubated with 15 μg of ^{35}S-labeled rUEV, and washed three times, and the radioactivity remaining in the cells was measured (column Pre at the far right in panels A to D). Control values in the absence of inhibitor ranged from 430 to 2,800 cpm. Experiments were performed in triplicate and were reproduced at least twice. The plotted data represent the means (error bars, standard deviation ranges).

The binding profile differs between undifferentiated and differentiated Caco-2 cells. White et al. reported that rNV/68 was able to bind more significantly to D-Caco-2 cells than to any other mammalian cell lines tested, although the cell surface binding factor was unknown (80). To assess the contribution of heparan sulfate glycosaminoglycan in the process of rUEV binding to Caco-2 cells, we investigated the binding of GI NV and GII NV to Caco-2 cells using a virus-binding assay. We prepared ^{35}S-labeled VLPs from four NV strains and compared the efficiencies of each strain in terms of ability to bind to undifferentiated Caco-2 (U-Caco-2) cells and to D-Caco-2 cells.

As depicted in Fig. 6A, the GI NV and GII NV strains differed greatly in terms of their ability to bind to U-Caco-2 cells. In contrast, the level of binding to D-Caco-2 cells did not differ significantly between the two genogroups, although slight differences between strains were observed (Fig. 6B). To determine whether or not cell surface heparan sulfate is necessary for this type of binding, we treated U-Caco-2 and D-Caco-2 cells with heparinase and measured the level of binding of ^{35}S-labeled rUEV to these cells. Digestion with heparinase I resulted in a dose-dependent reduction of up to 90% in the case of binding to U-Caco-2 cells (Fig. 6C). However, the corresponding reduction with heparinase I amounted to only 50% in the case of the D-Caco-2 cells (Fig. 6D), indicating that although heparan sulfate is the major binding molecule for U-Caco-2 cells, it contributed to only half of the amount of binding in the case of the D-Caco-2 cells.

Contribution of H-type blood antigen to rUEV binding to D-Caco-2 cells. A recent study has shown that D-Caco-2 cells have a high level of expression of H-type 1 blood group antigen on the cell surface (2). Other related studies have suggested that rNV/68 is associated with H-type histo-blood antigen (32, 49). Therefore, we investigated the inhibitory activity of the blood group H disaccharide, blood group A trisaccharide, and blood group B trisaccharide. As depicted in Fig. 7A, only incubation of ^{35}S-labeled rUEV with blood group H disaccharide reduced the binding to D-Caco-2 cells by more than 40%. Next, we used α1,2-fucosidase to determine whether the 1,2-fucosylated structure was important for NV binding (49). Pretreatment of D-Caco-2 cells with α1,2-fucosidase also dose dependently reduced the amount of binding by approximately

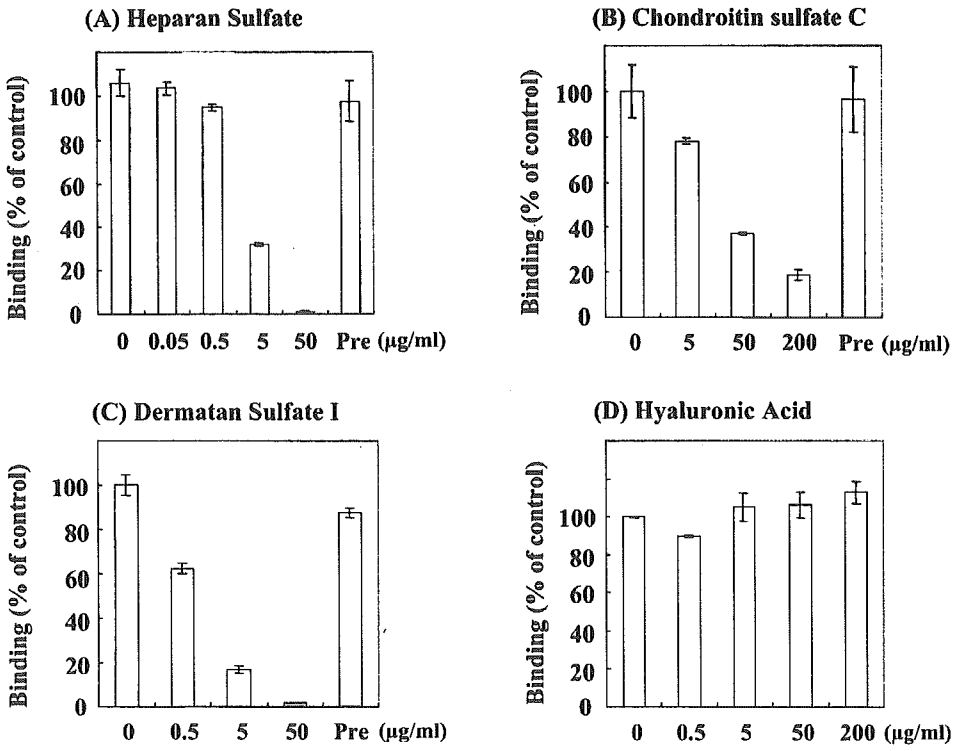

FIG. 3. Inhibition of binding of rUEV by glycosaminoglycans. Intestine 407 cell monolayers were incubated with ^{35}S-labeled rUEV in the presence of increasing concentrations of each glycosaminoglycan: heparan sulfate (A), chondroitin sulfate C (B), dermatan sulfate I (C), and hyaluronic acid (D). The cells were also preincubated with each glycosaminoglycan at a concentration of 50 μg/ml, washed three times, incubated with 15 μg of ^{35}S-labeled rUEV, and washed three times, and the radioactivity of the cells was measured (column Pre at the far right in panels A to C). Control values in the absence of the glycosaminoglycan ranged from 570 to 1,270 cpm. The experiments were performed in triplicate and were reproduced at least twice. The plotted data represent the means (error bars, standard deviation ranges).

40% (Fig. 7B). These experiments indicated that approximately half of the bound rUEV was associated with heparan sulfate and the other half was associated with H-type blood group antigen on the D-Caco-2 cells (Fig. 6D and Fig. 7). Although it remains unclear whether rUEV could bind to blood group A antigen or blood group B antigen based on this assay, our data suggested that rUEV particles probably possess separate binding sites for at least heparan sulfate and H-type blood antigen.

Cell surface heparan sulfate for rUEV binding to various cells. To determine whether the interaction between rUEV and heparan sulfate is limited to Intestine 407 and Caco-2 cells (Fig. 4 and 6), we treated five cell lines derived from different species with heparinase I and measured the extent of rUEV binding (Fig. 8). Digestion with heparinase I (20 U/ml) resulted in a marked reduction in binding to all five cell lines, although the degree of binding to Tn5 insect cells was relatively high (Fig. 8). These results suggested that the interaction between rUEV and heparan sulfate is ubiquitously shared by cells from various species, although the structure of heparan sulfate differs from tissue to tissue and species to species (14, 72).

Cell surface heparan sulfate for GI NV binding. To determine whether the weak binding of GI VLPs to cells is associated with cell surface heparan sulfate (Fig. 1), we performed binding assays in the presence of heparin and also after treatment with heparinase I (Fig. 9). The inhibitory effects of heparin differed in a comparison of the GI and the GII NVs (Fig. 2A), although the binding of rSEV and rFUV to Intestine 407 cells decreased in both cases in a dose-dependent manner, respectively (Fig. 9). No inhibition was observed when the cells were pretreated with heparin at 2.5 μg/ml (Fig. 9). Digestion with heparinase I (20 U/ml) resulted in an incomplete reduction of the binding of ^{35}S-labeled rSEV and rFUV (~60 and ~40%, respectively) (Fig. 9). These results suggested that the cell surface heparan sulfate glycosaminoglycan might not be the major molecule involved in the binding process of at least two strains of GI NV.

DISCUSSION

Heparan sulfate, a long polyanionic carbohydrate chain consisting of repeating disaccharides, is found in a wide variety of tissues in many animal species (14, 73). This molecule has a core protein that is rooted in the lipid bilayer of the plasma membrane of most types of vertebrate and invertebrate cells (41, 51). A number of studies have indicated the potential roles of heparan sulfate proteoglycans in the regulation of cell growth and transformation (15, 61, 77, 84), differentiation processes (10), cell adhesion (12, 44), and neuromuscular junction formation (3). In addition, heparan sulfate acts as a receptor,

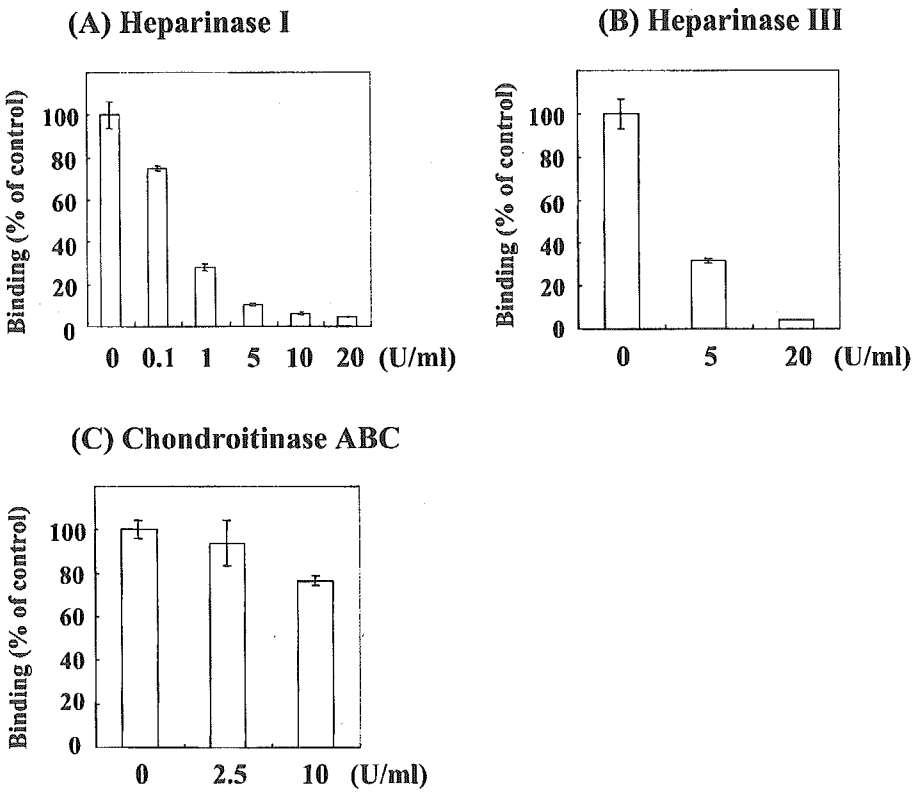

FIG. 4. Effect of treatment with lyase on binding. Intestine 407 cell monolayers were pretreated with increasing concentrations of each enzyme for 1 h, and the binding of ^{35}S-labeled rUEV was measured. Control values in the absence of the enzyme ranged from 1,050 to 1,520 cpm. The experiments were performed in triplicate and were reproduced at least twice. The plotted data represent the means (error bars, standard deviation ranges). (A) Heparinase I (0 to 20 U/ml); (B) heparinase III (0 to 20 U/ml); (C) chondroitinase ABC (0 to 10 U/ml).

not only for viruses, but also for bacteria and parasites (11, 62, 65, 69).

Our series of experiments demonstrated that rUEV and rCHV, recombinant VLPs from GII NV, predominantly bound to heparan sulfate on most mammalian cell surfaces tested, except for on D-Caco-2 cells. The first indication leading to our present conclusions was obtained from experiments using the binding inhibitors heparin and suramin. These molecules had been shown to block the binding of rUEV to Intestine 407 cells by associating with the VLPs and not with the cells. The binding to rUEV presumably occurred via the sulfated portion of these inhibitors, which occupied the sites on the VLPs that were otherwise necessary for binding to cell surface heparan sulfate (Fig. 2A and B). Heparin, a functional analogue of heparan sulfate, is a polymer containing repeated disaccharides and suramin, a complex derivative of urea. Other than their respective sulfate groups, there was no other common feature shared by these two molecules. Unexpectedly, chondroitin sulfate C and dermatan sulfate I also exerted inhibitory effects on binding at higher doses (Fig. 3B), which is a finding that differs from that in studies of dengue virus; the discrepancy is due to the fact that these two compounds had no inhibitory effect on dengue virus. The binding of dengue virus was exclusively blocked by highly sulfated heparan sulfate (11). Poly-L-lysine and protamine sulfate directly inhibited the binding of rUEV to Intestine 407 cells by associating with the cell surface (Fig. 2C and D). The binding of heparan sulfate, chondroitin sulfate C, and dermatan sulfate I to rUEV is thought to be due to their glycosaminoglycan-specific structures, such as sulfated sugars, rather than being the result of a simple nonspecific effect, since hyaluronic acid did not show any inhibitory effect, even at doses up to 200 μg/ml. In contrast with all other glycosaminoglycans, hyaluronic acid contains no sulfated sugars (27). Under the present assay conditions, Intestine 407 cell surface heparan sulfate was shown to be associated with more than 90% of the binding that took place, as indicated by treatment with heparinase I or III at 20 U/ml (Fig. 4A and B). NV presumably interacts with other cell surface glycosaminoglycans in vivo; for instance, chondroitin sulfate exists abundantly in the human intestinal tract (73).

Removal of heparan sulfate by heparinase III, a heparan sulfate-specific enzyme, clearly indicated that this molecule is specifically associated with the binding between Intestine 407 cells and rUEV (Fig. 4B). Although rUEV selectively binds to heparan sulfate on Intestine 407 cells, we cannot rule out the possibility that rUEV interacted with other cell surface polyanions. In a previous study, we suggested a 105-kDa protein as a candidate receptor molecule in various mammalian cells (71), but this 105-kDa molecule did not correspond to cell surface heparan sulfate (data not shown).

The sulfation of heparan sulfate is important for the binding of rUEV to Intestine 407 cells, as shown in Fig. 5. These results

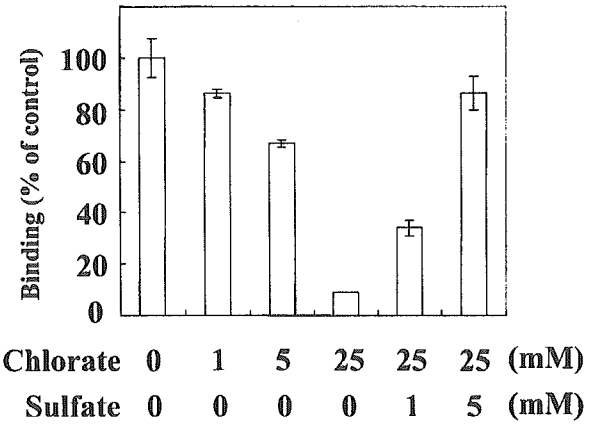

FIG. 5. Effect of sulfation of glycosaminoglycan in the binding of rUEV. Vero cells were incubated in the presence of increasing concentrations (0, 1, 5, and 25 mM) of sodium chlorate. After the cells were washed, the binding of ^{35}S-labeled rUEV was examined. Cells incubated in the presence of 25 mM sodium chlorate were supplemented with either 1 or 5 mM sodium sulfate for 48 h. After the cells were washed, the binding of ^{35}S-labeled rUEV was measured. The experiments were performed in triplicate and were reproduced at least twice. The plotted data represent the means (error bars, standard deviation ranges).

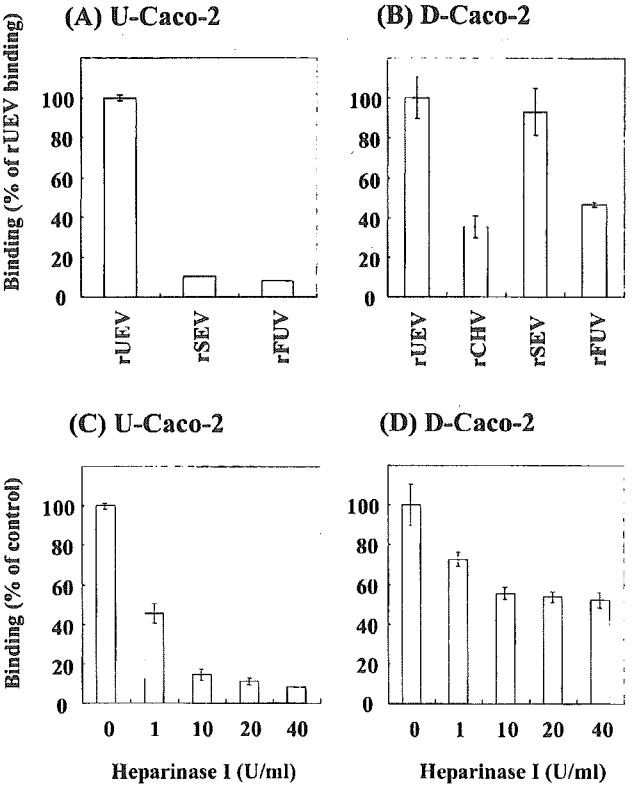

FIG. 6. Comparison of binding of VLPs to U-Caco-2 and D-Caco-2 cells. Fifteen micrograms of ^{35}S-labeled VLPs was incubated with either U-Caco-2 or D-Caco-2 cells for 1 h at 4°C. After the cells were washed, the binding of VLPs to the cells was measured. (A) U-Caco-2 cells were incubated with ^{35}S-labeled rUEV, rSEV, and rFUV. (B) D-Caco-2 cells were incubated with ^{35}S-labeled rUEV, rCHV, rSEV, and rFUV. The effect of heparinase I treatment on the binding of rUEV to U-Caco-2 and D-Caco-2 cells was also measured. Monolayers of U-Caco-2 (C) and D-Caco-2 (D) were pretreated with increasing concentrations of heparinase I for 1 h before 15 μg of ^{35}S-labeled rUEV was added. After washing, the radioactivity of the cells was measured. The experiments were performed in triplicate and were reproduced at least twice. The plotted data represent the means (error bars, standard deviation ranges).

may explain the inhibition by suramin, a compound not related structurally to glycosaminoglycans but one that contains six sulfate groups (Fig. 2B). Recent studies have shown that the structure of heparan sulfate is highly heterogeneous in terms of both the pattern and level of sulfation, as well as in terms of the primary sequence of disaccharides, depending on the tissues and species from which this molecule is extracted (48, 72). Such differences may explain the tropism of pathogenic microorganisms that exploit heparan sulfate structures as a target for binding (11). In our previous study, we did not observe an association of rUEV with glycoproteins, since the binding of rUEV was not influenced by treatment with sodium periodate (71). We are of the opinion that oxidation by sodium periodate is unlikely to affect the sulfate group of heparan sulfate (16).

Although heparan sulfate appeared to play a role in the binding of rUEV to Intestine 407 cells, the structure of heparan sulfate is known to be heterogeneous, depending on the cell type (51, 73). Therefore, U-Caco-2, CHO, HeLa, A549, and Vero cells were digested with heparinase I, and the subsequent extent of rUEV binding was examined. As indicated in Fig. 8, treatment with enzymes drastically reduced the extent of binding, indicating that heparan sulfate was also used for the binding process in these other types of cell. However, the binding of rUEV to D-Caco-2 (Fig. 6D) and Tn5 (Fig. 8) cells reflected some degree of resistance to heparinase I digestion. These results therefore suggest that a cell surface molecule(s) other than heparan sulfate participated in the binding process in these cases.

A difference in the binding efficiency was detected between GI and GII VLPs, whereby GI VLPs were found to inefficiently bind to the cells, when they were compared to GII VLPs (Fig. 1). A low level of binding of rSEV and rFUV was observed, compared with that of GII VLPs (Fig. 1A), and the inhibition by both heparin and heparinase I was only half complete (Fig. 9). A similar incomplete inhibitory effect was observed in the case of treatment with suramin (data not shown). Therefore, we concluded that both rSEV and rFUV also bind to cell surface heparan sulfate very weakly or nonspecifically. This finding may account for previous data by White et al. that NV/68 did not bind to most cell lines, with the exception of Caco-2 cells (80). Most human cell lines used in their assay would have expressed heparan sulfate proteoglycan on the cell surface. However, GI NV is likely to bind to heparan sulfate nonspecifically, which would result in a low level of binding to those cell lines. As regards the binding to insect Sf9 cells, NV/68 possibly bound to molecules other than heparan sulfate, as was observed in our experiments with another insect cell, Tn5 (Fig. 8). It is of note in this context that the hemagglutination profiles of GI and GII were also different (32).

Generally, binding assays are typically carried out at 4°C in order to avoid changes in physiological conditions. However, most viruses infect human hosts at body temperature, 37°C, in

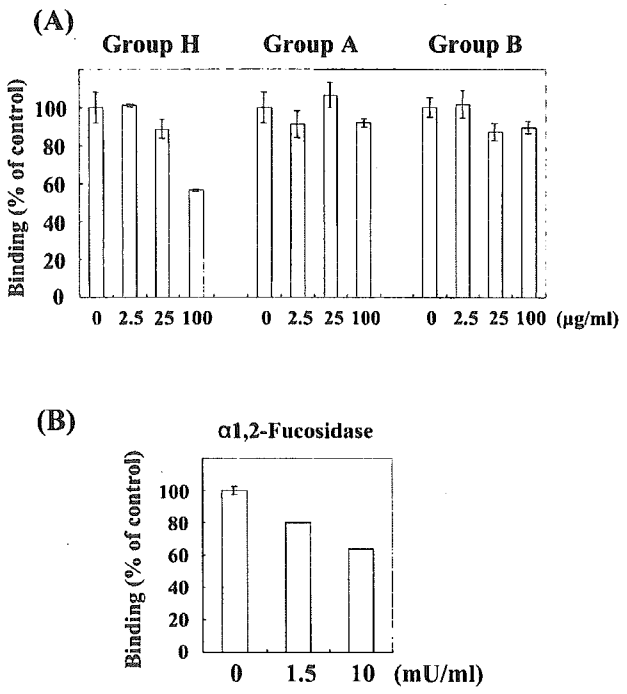

FIG. 7. Blood antigens on binding of rUEV to D-Caco-2 cells. (A) D-Caco-2 cell monolayers were incubated with ^{35}S-labeled rUEV in the presence of increasing concentrations (1 to 100 μg/ml) of blood group H disaccharide, blood group A trisaccharide, or blood group B trisaccharide. The cells were washed, and the radioactivity of the cells was measured. (B) D-Caco-2 cell monolayers were pretreated with increasing concentrations (0 to 10 mU/ml) of α1,2-fucosidase for 1 h at 37°C before 15 μg of ^{35}S-labeled rUEV was added. The radioactivity of the cells was then measured. Control values in the absence of the enzyme ranged from 190 to 710 cpm. The experiments were performed in triplicate and were reproduced at least twice. The plotted data represent the means (error bars, standard deviation ranges).

vivo. Interestingly, ^{35}S-labeled rUEV associated equally to Intestine 407 and CHO cells at both 4 and 37°C (data not shown). In contrast, ^{35}S-labeled rUEV bound neither to U-Caco-2 nor D-Caco-2 cells at 37°C (data not shown). In early studies using coxsackievirus B3 and poliovirus, more than 50% of the cell-

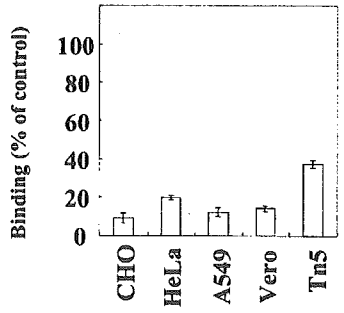

FIG. 8. Heparinase I treatment of several cell lines and the binding of rUEV. CHO, HeLa, A549, Vero, and Tn5 cell monolayers were pretreated with heparinase I (20 U/ml) for 1 h, and 15 μg of ^{35}S-labeled rUEV was added. After the cells were washed, the radioactivity of the cells was measured. The experiments were performed in triplicate and were reproduced at least twice. The plotted data represent the means (error bars, standard deviation ranges).

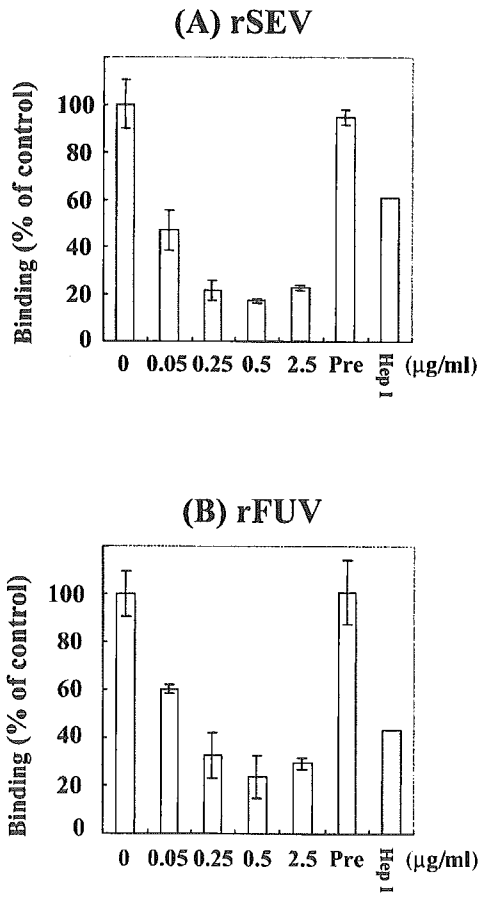

FIG. 9. Effects of heparin and heparinase I on GI VLP adsorption to Intestine 407 cells. Intestine 407 cell monolayers were incubated with ^{35}S-labeled rSEV (A) or ^{35}S-labeled rFUV (B) in the presence of increasing concentrations (0, 0.05, 0.25, 0.5, and 2.5 μg/ml) of heparin. Cells were also preincubated with heparin at a concentration of 2.5 μg/ml before being incubated with 15 μg of ^{35}S-labeled rSEV (A) or ^{35}S-labeled rFUV (B), and the radioactivity of the cells was measured (columns labeled Pre). In another experiment, the cells were treated with heparinase I (20 U/ml) for 1 h before 15 μg of ^{35}S-labeled rSEV (A) or ^{35}S-labeled rFUV (B) was added (Hep I). Control values in the absence of heparin or the enzyme ranged from 80 to 95 cpm. The experiments were performed in triplicate and were reproduced at least twice. The plotted data represent the means (error bars, standard deviation ranges).

associated viruses were shown to be eluted from the cells at 37°C (13, 35), and a recent kinetic analysis suggested that the poliovirus receptor functions like an enzyme (74). These observations raised two different possibilities regarding the interaction between heparan sulfate and VLPs: (i) heparan sulfate is only activated in the company of a Caco-2 cell-specific component, or (ii) the temperature sensitivity of heparan sulfate glycosaminoglycan of Caco-2 cells differs from that of other cell lines. Some ligand-heparan sulfate interactions require a particular structure of heparan sulfate (11). Further investigation will be required to resolve this issue.

In this study, we demonstrated that cell surface heparan sulfate could efficiently associate with GII NV. Intestinal glycosaminoglycans are likely to be associated with NV infection,

since abundant glycosaminoglycans are observed in the human intestine (73). It is also likely that the binding of NV to glycosaminoglycans serves merely to concentrate the virus on the cell surface, such that binding to another receptor is facilitated (81). Alternatively, the binding of a virion component with glycosaminoglycans is necessary for a virion-cell interaction, e.g., the interactions observed in neural cells (12, 84). It is unclear whether heparan sulfate functions as the NV receptor, because the expression of heparan sulfate does not always support viral infection (54, 68). Further investigation will be needed to identify the NV receptor.

In a recent study, we found that histone H1 inhibits the binding of NV VLPs to the mammalian cell surface by associating with both VLPs and the cell surface (70). Various interactions between histones and the glycosaminoglycans in the nuclei and those on the cell surface have been described (8, 9, 17, 76, 79). Such findings, in combination with our data, suggest that histone H1 may directly bind cell surface heparan sulfate and consequently block the binding of NV to the cell surface.

ACKNOWLEDGMENTS

We thank Y. Matsuura (Osaka University), T. Matsukura (NIID), and T. Shimada (Tokyo University) for helpful discussions and suggestions. We also thank T. Mizoguchi, M. Matsuda, M. Yahata, and S. Yoshizaki for their secretarial work and technical support. We are grateful to N. Sakurai, S. Kobayashi, and K. Shinozaki for providing the UEV, CHV, SEV, and FUV.

This study was supported by a grant for Research on Emerging and Reemerging Infectious Diseases from the Ministry of Health, Labor and Welfare to N. Takeda. M. Tamura received the support of a Research Fellowship from the Japan Society for the Promotion of Science for Young Scientists.

REFERENCES

1. **Adler, J. L., and R. Zickl.** 1969. Winter vomiting disease. J. Infect. Dis. **119**:668–673.
2. **Amano, J., and M. Oshima.** 1999. Expression of the H type 1 blood group antigen during enterocytic differentiation of Caco-2 cells. J. Biol. Chem. **274**:21209–21216.
3. **Anderson, M. J., F. G. Klier, and K. E. Tanguay.** 1984. Acetylcholine receptor aggregation parallels the deposition of a basal lamina proteoglycan during development of the neuromuscular junction. J. Cell Biol. **99**:1769–1784.
4. **Ando, T., J. S. Noel, and R. L. Fankhauser.** 2000. Genetic classification of "Norwalk-like viruses." J. Infect. Dis. **181**:S336–S348.
5. **Baeuerle, P. A., and W. B. Huttner.** 1986. Chlorate—a potent inhibitor of protein sulfation in intact cells. Biochem. Biophys. Res. Commun. **141**:870–877.
6. **Ball, J. M., M. E. Hardy, R. L. Atmar, M. E. Conner, and M. K. Estes.** 1998. Oral immunization with recombinant Norwalk virus-like particles induces a systemic and mucosal immune response in mice. J. Virol. **72**:1345–1353.
7. **Basavappa, R., A. Gomez-Yafal, and J. M. Hogle.** 1998. The poliovirus empty capsid specifically recognizes the poliovirus receptor and undergoes some, but not all, of the transitions associated with cell entry. J. Virol. **72**:7551–7556.
8. **Bilozur, M. E., and C. Biswas.** 1990. Identification and characterization of heparan sulfate-binding proteins from human lung carcinoma cells. J. Biol. Chem. **265**:19697–19703.
9. **Bornens, M.** 1973. Action of heparin on nuclei: solubilization of chromatin enabling the isolation of nuclear membranes. Nature **244**:28–30.
10. **Cassaro, C. M. F., and C. P. Dietrich.** 1977. Distribution of sulfated mucopolysaccharides in invertebrates. J. Biol. Chem. **252**:2254–2261.
11. **Chen, Y., T. Maguire, R. E. Hileman, J. R. Fromm, J. D. Esko, R. J. Linhardt, and R. M. Marks.** 1997. Dengue virus infectivity depends on envelope protein binding to target cell heparan sulfate. Nat. Med. **3**:866–871.
12. **Cole, G. J., A. Loewy, and L. Glaser.** 1986. Neuronal cell-cell adhesion depends on interactions of N-CAM with heparin-like molecules. Nature **320**:445–447.
13. **Crowell, R. L., and L. Philipson.** 1971. Specific alterations of coxsackievirus B3 eluted from HeLa cells. J. Virol. **8**:509–515.
14. **Dietrich, C. P., H. B. Nader, and A. H. Straus.** 1983. Structural differences of heparan sulfates according to the tissue and species of origin. Biochem. Biophys. Res. Commun. **111**:865–871.
15. **Esko, J. D., K. S. Rostand, and J. L. Weinke.** 1988. Tumor formation dependent on proteoglycan biosynthesis. Science **241**:1092–1096.
16. **Fransson, L. A., I. Sjoberg, and B. Havsmark.** 1980. Structural studies on heparan sulphates. Characterization of oligosaccharides; obtained by periodate oxidation and alkaline elimination. Eur. J. Biochem. **106**:59–69.
17. **Frenster, J. H.** 1965. Nuclear polyanions as de-repressors of synthesis of ribonucleic acid. Nature **206**:680–683.
18. **Glass, P. J., L. J. White, J. M. Ball, I. Leparc-Goffart, M. E. Hardy, and M. K. Estes.** 2000. Norwalk virus open reading frame 3 encodes a minor structural protein. J. Virol. **74**:6581–6591.
19. **Gray, J. J., X. Jiang, P. Morgan-Capner, U. Desselberger, and M. K. Estes.** 1993. Prevalence of antibodies to Norwalk virus in England: detection by enzyme-linked immunosorbent assay using baculovirus-expressed Norwalk virus capsid antigen. J. Clin. Microbiol. **31**:1022–1025.
20. **Green, K. Y.** 2000. Summary of the first international workshop on human caliciviruses. J. Infect. Dis. **181**:S252–S253.
21. **Green, K. Y., R. M. Chanock, and A. Z. Kapikian.** 2001. Human caliciviruses, p. 841–874. *In* D. M. Knipe and P. M. Howley (ed.), Fields virology, vol. 1. Lippincott Williams & Wilkins, Philadelphia, Pa.
22. **Green, K. Y., J. F. Lew, X. Jiang, A. Z. Kapikian, and M. K. Estes.** 1993. Comparison of the reactivities of baculovirus-expressed recombinant Norwalk virus capsid antigen with those of the native Norwalk virus antigen in serologic assays and some epidemiologic observations. J. Clin. Microbiol. **31**:2185–2191.
23. **Greenberg, H. B., J. Valdesuso, R. H. Yolken, E. Gangarosa, W. Gary, R. G. Wyatt, T. Konno, H. Suzuki, R. M. Chanock, and A. Z. Kapikian.** 1979. Role of Norwalk virus in outbreaks of nonbacterial gastroenteritis. J. Infect. Dis. **139**:564–568.
24. **Griffin, M. R., J. J. Surowiec, D. I. McCloskey, B. Capuano, B. Pierzynski, M. Quinn, R. Wojnarski, W. E. Parkin, H. Greenberg, and G. W. Gary.** 1982. Foodborne Norwalk virus. Am. J. Epidemiol. **115**:178–184.
25. **Grohmann, G. S., A. M. Murphy, P. J. Christopher, E. Auty, and H. B. Greenberg.** 1981. Norwalk virus gastroenteritis in volunteers consuming depurated oysters. Aust. J. Exp. Biol. Med. Sci. **59**:219–228.
26. **Guerrero, R. A., J. M. Ball, S. S. Krater, S. E. Pacheco, J. D. Clements, and M. K. Estes.** 2001. Recombinant Norwalk virus-like particles administered intranasally to mice induce systemic and mucosal (fecal and vaginal) immune responses. J. Virol. **75**:9713–9722.
27. **Hardingham, T. E., and A. J. Fosang.** 1992. Proteoglycans: many forms and many functions. FASEB J. **6**:861–870.
28. **Harrington, P. R., L. Lindesmith, B. Yount, C. L. Moe, and R. S. Baric.** 2002. Binding of Norwalk virus-like particles to ABH histo-blood group antigens is blocked by antisera from infected human volunteers or experimentally vaccinated mice. J. Virol. **76**:12335–12343.
29. **Hedman, K., M. Kurkinen, K. Alitalo, A. Vaheri, S. Johansson, and M. Hook.** 1979. Isolation of the pericellular matrix of human fibroblast cultures. J. Cell Biol. **81**:83–91.
30. **Hink, W. F.** 1970. Establish insect cell line from the cabbage looper, Trichoplusia ni. Nature **226**:466–467.
31. **Hutson, A. M., R. L. Atmar, D. Y. Graham, and M. K. Estes.** 2002. Norwalk virus infection and disease is associated with ABO histo-blood group type. J. Infect. Dis. **185**:1335–1337.
32. **Hutson, A. M., R. L. Atmar, D. M. Marcus, and M. K. Estes.** 2003. Norwalk virus-like particle hemagglutination by binding to H histo-blood group antigens. J. Virol. **77**:405–415.
33. **Jiang, X., D. Y. Graham, K. Wang, and M. K. Estes.** 1990. Norwalk virus genome cloning and characterization. Science **250**:1580–1583.
34. **Jiang, X., M. Wang, D. Y. Graham, and M. K. Estes.** 1992. Expression, self-assembly, and antigenicity of the Norwalk virus capsid protein. J. Virol. **66**:6527–6532.
35. **Joklik, W. K., and J. E. Darnell, Jr.** 1961. The adsorption and early fate of purified poliovirus in HeLa cells. Virology **13**:439–447.
36. **Kanwar, Y. S., and M. G. Farquhar.** 1979. Presence of heparan sulfate in the glomerular basement membrane. Proc. Natl. Acad. Sci. USA **76**:1303–1307.
37. **Kapikian, A. Z., R. G. Wyatt, R. Dolin, T. S. Thornhill, A. R. Kalica, and R. M. Chanock.** 1972. Visualization by immune electron microscopy of a 27-nm particle associated with acute infectious nonbacterial gastroenteritis. J. Virol. **10**:1075–1081.
38. **Kaplan, J. E., G. W. Gary, R. C. Baron, N. Singh, L. B. Schonberger, R. Feldman, and H. B. Greenberg.** 1982. Epidemiology of Norwalk gastroenteritis and the role of Norwalk virus in outbreaks of acute nonbacterial gastroenteritis. Ann. Intern. Med. **96**:756–761.
39. **Kaplan, J. E., R. A. Goodman, L. B. Schonberger, E. C. Lippy, and G. W. Gary.** 1982. Gastroenteritis due to Norwalk virus: an outbreak associated with a municipal water system. J. Infect. Dis. **146**:190–197.
40. **Katayama, K., H. Shirato-Horikoshi, S. Kojima, T. Kageyama, T. Oka, F. Hoshino, S. Fukushi, M. Shinohara, K. Uchida, Y. Suzuki, T. Gojobori, and N. Takeda.** 2002. Phylogenetic analysis of the complete genome of 18 Norwalk-like viruses. Virology **299**:225–239.
41. **Kjellen, L., I. Pettersson, and M. Hook.** 1981. Cell-surface heparan sulfate:

an intercalated membrane proteoglycan. Proc. Natl. Acad. Sci. USA **78:** 5371–5375.
42. **Kobayashi, S., K. Sakae, Y. Suzuki, H. Ishiko, K. Kamata, K. Suzuki, K. Natori, T. Miyamura, and N. Takeda.** 2000. Expression of recombinant capsid proteins of chitta virus, a genogroup II Norwalk virus, and development of an ELISA to detect the viral antigen. Microbiol. Immunol. **44:**687–693.
43. **Kobayashi, S., K. Sakae, Y. Suzuki, K. Shinozaki, M. Okada, H. Ishiko, K. Kamata, K. Suzuki, K. Natori, T. Miyamura, and N. Takeda.** 2000. Molecular cloning, expression, and antigenicity of Seto virus belonging to genogroup I Norwalk-like viruses. J. Clin. Microbiol. **38:**3492–3494.
44. **Laterra, J., J. E. Silbert, and L. A. Culp.** 1983. Cell surface heparan sulfate mediates some adhesive responses to glycosaminoglycan-binding matrices, including fibronectin. J. Cell Biol. **96:**112–123.
45. **Lew, J. F., A. Z. Kapikian, J. Valdesuso, and K. Y. Green.** 1994. Molecular characterization of Hawaii virus and other Norwalk-like viruses: evidence for genetic polymorphism among human caliciviruses. J. Infect. Dis. **170:**535–542.
46. **Lindesmith, L., C. Moe, S. Marionneau, N. Ruvoen, X. Jiang, L. Lindblad, P. Stewart, J. Le Pendu, and R. Baric.** 2003. Human susceptibility and resistance to Norwalk virus infection. Nat. Med. **9:**548–553.
47. **Lohse, D. L., and R. J. Linhardt.** 1992. Purification and characterization of heparin lyases from *Flavobacterium heparinum*. J. Biol. Chem. **267:**24347–24355.
48. **Maccarana, M., Y. Sakura, A. Tawada, K. Yoshida, and U. Lindahl.** 1996. Domain structure of heparan sulfates from bovine organs. J. Biol. Chem. **271:**17804–17810.
49. **Marionneau, S., N. Ruvoen, B. Le Moullac-Vaidye, M. Clement, A. Cailleau-Thomas, G. Ruiz-Palacois, P. Huang, X. Jiang, and J. Le Pendu.** 2002. Norwalk virus binds to histo-blood group antigens present on gastroduodenal epithelial cells of secretor individuals. Gastroenterology **122:**1967–1977.
50. **Mason, H. S., J. M. Ball, J. J. Shi, X. Jiang, M. K. Estes, and C. J. Arntzen.** 1996. Expression of Norwalk virus capsid protein in transgenic tobacco and potato and its oral immunogenicity in mice. Proc. Natl. Acad. Sci. USA **93:**5335–5340.
51. **Medeiros, G. F., A. Mendes, R. A. B. Castro, E. C. Bau, H. B. Nader, and C. P. Dietrich.** 2000. Distribution of sulfated glycosaminoglycans in the animal kingdom: widespread occurrence of heparin-like compounds in invertebrates. Biochim. Biophys. Acta **1475:**287–294.
52. **Meeroff, J. C., D. S. Schreiber, J. S. Trier, and N. R. Blacklow.** 1980. Abnormal gastric motor function in viral gastroenteritis. Ann. Intern. Med. **92:**370–373.
53. **Mitsuya, H., D. J. Looney, S. Kuno, R. Ueno, F. Wong-Staal, and S. Broder.** 1988. Dextran sulfate suppression of viruses in the HIV family: inhibition of virion binding to CD4+ cells. Science **240:**646–649.
54. **Montgomery, R. I., M. S. Warner, B. J. Lum, and P. G. Spear.** 1996. Herpes simplex virus-1 entry into cells mediated by a novel member of the TNF/NGF receptor family. Cell **87:**427–436.
55. **Morse, D. L., J. J. Guzewich, J. P. Hanrahan, R. Stricof, M. Shayegani, R. Deibel, J. C. Grabau, N. A. Nowak, J. E. Herrmann, G. Cukor, and N. R. Blacklow.** 1986. Widespread outbreaks of clam- and oyster-associated gastroenteritis. Role of Norwalk virus. N. Engl. J. Med. **314:**678–681.
56. **Nader, H. B., C. P. Dietrich, V. Buonassisi, and P. Colburn.** 1987. Heparin sequences in the heparan sulfate chains of an endothelial cell proteoglycan. Proc. Natl. Acad. Sci. USA **84:**3565–3569.
57. **Parrino, T. A., D. S. Schreiber, J. S. Trier, A. Z. Kapikian, and N. R. Blacklow.** 1977. Clinical immunity in acute gastroenteritis caused by Norwalk agent. N. Engl. J. Med. **297:**86–89.
58. **Payne, E., M. R. Bowles, A. Don, J. F. Hancock, and N. A. J. McMillan.** 2001. Human papillomavirus type 6b virus-like particles are able to activate the Ras-MAP kinase pathway and induce cell proliferation. J. Virol. **75:**4150–4157.
59. **Prasad, B. V. V., M. E. Hardy, T. Dokland, J. Bella, M. G. Rossmann, and M. K. Estes.** 1999. X-ray crystallographic structure of the Norwalk virus capsid. Science **286:**287–290.
60. **Prasad, B. V. V., R. Rothnagel, X. Jiang, and M. K. Estes.** 1994. Three-dimensional structure of baculovirus-expressed Norwalk virus capsids. J. Virol. **68:**5117–5125.
61. **Roberts, R., J. Gallagher, E. Spooncer, T. D. Allen, F. Bloomfield, and T. M. Dexter.** 1988. Heparan sulphate bound growth factors: a mechanism for stromal cell mediated haemopoiesis. Nature **332:**376–378.
62. **Rostand, K. S., and J. D. Esko.** 1997. Microbial adherence to and invasion through proteoglycans. Infect. Immun. **65:**1–8.
63. **Schreiber, D. S., N. R. Blacklow, and J. S. Trier.** 1973. The mucosal lesion of the proximal small intestine in acute infectious nonbacterial gastroenteritis. N. Engl. J. Med. **288:**1318–1323.
64. **Schreiber, D. S., N. R. Blacklow, and J. S. Trier.** 1974. The small intestinal lesion induced by Hawaii agent acute infectious nonbacterial gastroenteritis. J. Infect. Dis. **129:**705–708.
65. **Shukla, D., J. Liu, P. Blaiklock, N. W. Shworak, X. Bai, J. D. Esko, G. H. Cohen, R. J. Eisenberg, R. D. Rosenberg, and P. G. Spear.** 1999. A novel role for 3-*O*-sulfated heparan sulfate in herpes simplex virus 1 entry. Cell **99:**13–22.
66. **Steiner, H., D. Hultmark, A. Engstrom, H. Bennich, and H. G. Boman.** 1981. Sequence and specificity of two antibacterial proteins involved in insect immunity. Nature **292:**246–248.
67. **Subekti, D. S., P. Tjaniadi, M. Lesmana, J. McArdle, D. Iskandriati, I. N. Budiarsa, P. Walujo, I. H. Suparto, I. Winoto, J. R. Campbell, K. R. Porter, D. Sajuthi, A. A. Ansari, and B. A. Oyofo.** 2002. Experimental infection of Macaca nemestrina with a Toronto Norwalk-like virus of epidemic viral gastroenteritis. J. Med. Virol. **66:**400–406.
68. **Subramanian, G., D. S. McClain, A. Perez, and A. O. Fuller.** 1994. Swine testis cells contain functional heparan sulfate but are defective in entry of herpes simplex virus. J. Virol. **68:**5667–5676.
69. **Summerford, C., and R. J. Samulski.** 1998. Membrane-associated heparan sulfate proteoglycan is a receptor for adeno-associated virus type 2 virions. J. Virol. **72:**1438–1445.
70. **Tamura, M., K. Natori, M. Kobayashi, T. Miyamura, and N. Takeda.** 2003. Inhibition of attachment of virions of Norwalk virus to mammalian cells by soluble histone molecules. Arch. Virol. **148:**1659–1670.
71. **Tamura, M., K. Natori, M. Kobayashi, T. Miyamura, and N. Takeda.** 2000. Interaction of recombinant Norwalk virus particles with the 105-kilodalton cellular binding protein, a candidate receptor molecule for virus attachment. J. Virol. **74:**11589–11597.
72. **Toida, T., H. Yoshida, H. Toyoda, I. Koshiishi, T. Imanari, R. E. Hileman, J. R. Fromm, and R. J. Linhardt.** 1997. Structural differences and the presence of unsubstituted amino groups in heparan sulphates from different tissues and species. Biochem. J. **322:**499–506.
73. **Toledo, O. M. S., and C. P. Dietrich.** 1977. Tissue specific distribution of sulfated mucopolysaccharides in mammals. Biochim. Biophys. Acta **498:**114–122.
74. **Tsang, S. K., B. M. McDermott, V. R. Racaniello, and J. M. Hogle.** 2001. Kinetic analysis of the effect of poliovirus receptor on viral uncoating: the receptor as a catalyst. J. Virol. **75:**4984–4989.
75. **Vaheri, A.** 1964. Heparin and related polyionic substances as virus inhibitors. Acta Pathol. Microbiol. Scand. **171**(Suppl.)**:**S1–S98.
76. **Villeponteau, B.** 1992. Heparin increases chromatin accessibility by binding the trypsin-sensitive basic residues in histones. Biochem. J. **288:**953–958.
77. **Vlodavsky, I., J. Folkman, R. Sullivan, R. Fridman, R. Ishai-Michaeli, J. Sasse, and M. Klagsbrun.** 1987. Endothelial cell-derived basic fibroblast growth factor: synthesis and deposition into subendothelial extracellular matrix. Proc. Natl. Acad. Sci. USA **84:**2292–2296.
78. **Wang, J., X. Jiang, H. P. Madore, J. Gray, U. Desselberger, T. Ando, Y. Seto, I. Oishi, J. F. Lew, K. Y. Green, and M. K. Estes.** 1994. Sequence diversity of small, round-structured viruses in the Norwalk virus group. J. Virol. **68:**5982–5990.
79. **Watson, K., N. J. Gooderham, D. S. Davies, and R. J. Edwards.** 1999. Nucleosomes bind to cell surface proteoglycans. J. Biol. Chem. **274:**21707–21713.
80. **White, L. J., J. M. Ball, M. E. Hardy, T. N. Tanaka, N. Kitamoto, and M. K. Estes.** 1996. Attachment and entry of recombinant Norwalk virus capsids to cultured human and animal cell lines. J. Virol. **70:**6589–6597.
81. **WuDunn, D., and P. G. Spear.** 1989. Initial interaction of herpes simplex virus with cells is binding to heparan sulfate. J. Virol. **63:**52–58.
82. **Wyatt, R. G., H. B. Greenberg, D. W. Dalgard, W. P. Allen, D. L. Sly, T. S. Thornhill, R. M. Chanock, and A. Z. Kapikian.** 1978. Experimental infection of chimpanzees with the Norwalk agent of epidemic viral gastroenteritis. J. Med. Virol. **2:**89–96.
83. **Yamagata, T., H. Saito, O. Habuchi, and S. Suzuki.** 1968. Purification and properties of bacterial chondroitinases and chondrosulfatases. J. Biol. Chem. **243:**1523–1535.
84. **Yayon, A., M. Klagsbrun, J. D. Esko, P. Leder, and D. M. Ornitz.** 1991. Cell surface, heparin-like molecules are required for binding of basic fibroblast growth factor to its high affinity receptor. Cell **64:**841–848.
85. **Zasloff, M.** 1987. Magainins, a class of antimicrobial peptides from Xenopus skin: isolation, characterization of two active forms, and partial cDNA sequence of a precursor. Proc. Natl. Acad. Sci. USA **84:**5449–5453.

JOURNAL OF CLINICAL MICROBIOLOGY, Apr. 2003, p. 1548–1557 Vol. 41, No. 4
0095-1137/03/$08.00+0 DOI: 10.1128/JCM.41.4.1548–1557.2003

Broadly Reactive and Highly Sensitive Assay for Norwalk-Like Viruses Based on Real-Time Quantitative Reverse Transcription-PCR

Tsutomu Kageyama,[1]* Shigeyuki Kojima,[1] Michiyo Shinohara,[2] Kazue Uchida,[2] Shuetsu Fukushi,[1] Fuminori B. Hoshino,[1] Naokazu Takeda,[3] and Kazuhiko Katayama[3]

Section of Infectious Disease, R&D Center, BML, Kawagoe, Saitama 350-1101,[1] Saitama Institute of Public Health, Saitama, Saitama 338-0824,[2] and Department of Virus Diseases and Vaccine Control, National Institute of Infectious Diseases, Musashi-murayama, Tokyo 208-0011,[3] Japan

Received 15 April 2002/Returned for modification 28 September 2002/Accepted 6 January 2003

We have developed an assay for the detection of Norwalk-like viruses (NLVs) based on reverse transcription-PCR (RT-PCR) that is highly sensitive to a broad range of NLVs. We isolated virus from 71 NLV-positive stool specimens from 37 outbreaks of nonbacterial acute gastroenteritis and sequenced the open reading frame 1 (ORF1)-ORF2 junction region, the most conserved region of the NLV genome. The data were subjected to multiple-sequence alignment analysis and similarity plot analysis. We used the most conserved sequences that react with diverse NLVs to design primers and TaqMan probes for the respective genogroups of NLV, GI and GII, for use in a real-time quantitative RT-PCR assay. Our method detected NLV in 99% (80 of 81) of the stool specimens that were positive by electron microscopy, a better detection rate than with the two available RT-PCR methods. Furthermore, our new method also detected NLV in 20 of 28 stool specimens from the same NLV-related outbreaks that were negative for virus by electron microscopy. Our new assay is free from carryover DNA contamination and detects low copy numbers of NLV RNA. It can be used as a routine assay for diagnosis as well as for elucidation of the epidemiology of NLV infections.

The Norwalk-like viruses (NLVs), members of the family *Caliciviridae*, are major causes of acute nonbacterial gastroenteritis and a major public health concern. NLV infections often result from ingesting contaminated food (14, 30), such as oysters (4, 8) and water (3, 33), or by person-to-person transmission in semiclosed communities, such as hospitals (35), schools (20), nursing homes (18), and cruise ships (12).

The major obstacle in the laboratory diagnosis of NLV infection is the lack of a tissue culture system for propagating the viruses. Therefore, electron microscopy (EM) has been routinely used (5) to detect NLV particles in stool specimens. However, the sensitivity of EM detection is low, requiring at least 10^6 viral particles per ml of stool.

Reverse transcription-PCR (RT-PCR) has been increasingly used for detection of viruses and would be an attractive alternative for NLV detection. The key to an efficient RT-PCR assay is finding conserved sequences to use as PCR primers. The great sequence diversity of the NLV genome has made this a challenging undertaking. Primers for previous assays have been taken from open reading frame 1 (ORF1) of the RNA-dependent RNA polymerase (RdRp) gene (1, 2, 9, 13, 15, 26, 27, 31, 37) or from ORF2 of the capsid protein gene (6, 10, 11, 13, 28, 38, 39).

Recently, we reported genogroup-specific primer sequences in the capsid gene (21). With those primers, our assay had a higher detection rate and allowed further differentiation of strains when the PCR products were sequenced. However, not all EM-positive stool specimens were positive by this RT-PCR.

* Corresponding author. Mailing address: Section of Infectious Disease, R&D Center, BML, Matoba 1361-1, Kawagoe, Saitama 350-1101, Japan. Phone: 81-49-232-0440. Fax: 81-49-232-5480. E-mail: tkage@alk.co.jp.

In this study, we sought to improve the primers. We explored sequences at the ORF1-ORF2 junction, the most conserved region in the NLV genome (19), and established an NLV detection assay for routine use with real-time quantitative RT-PCR.

MATERIALS AND METHODS

Stool specimens and examination by EM. Stool specimens were obtained from 210 symptomatic individuals from 37 outbreaks of nonbacterial acute gastroenteritis in Saitama Prefecture, Japan, between January 1997 and March 2000. The outbreaks occurred in a variety of settings, including restaurants, nursery schools, hotels, schools, dormitories, residences, and a nursing home. All stool specimens were examined by EM. NLVs were identified as round granular particles with a diameter of ~35 nm, a ragged edge, and an amorphous surface appearance, according to described criteria (5). Screening by EM revealed NLV particles in 110 stool specimens from the 210 patients.

RNA extraction from stool specimens. A 10% (wt/vol) stool suspension was prepared with distilled sterile water and clarified by centrifugation at 3,000 × *g* for 20 min. Viral RNA was extracted from 140 μl of a 10% stool suspension with a QIAamp viral RNA kit (Qiagen, Valencia, Calif.) according to the manufacturer's instructions. RNAs were eluted with 60 μl of diethyl pyrocarbonate-treated water and kept at −80°C until used in RT.

PlotSimilarity analysis. We used the complete genome sequences of 14 NLVs. Five were previously described, including Nowalk/68 virus (16), Southampton virus (22), strain BS5 (32), Camberwell virus (34), and Lordsdale virus (7). Nine others resulted from our own work, including the NLV genogroup I (GI) strain SzUGI and the NLV GII strains Saitama U1, U3, U4, U16, U17, U18, U201, and U25 (19). These full-length sequences were analyzed to generate similarity plots with the PlotSimilarity program of the Wisconsin Sequence Analysis Package version 9 (Genetics Computer Group, Madison, Wis.).

Sequencing of the ORF1-ORF2 junction regions of NLVs. To amplify the NLV GI ORF1-ORF2 junction region, PCR was carried out with a mixture of three forward primers, G1FF (5′-ATHGAACGYCAAATYTTCTGGAC-3′, 5′-ATHGAAAGACAAATCTACTGGAC-3′, and 5′-ATHGARAGRCARCTNTGGTGGAC-3′, corresponding to nucleotides [nt] 5075 to 5097 in Norwalk/68), and a reverse primer, G1SKR (21). To amplify the NLV GII ORF1-ORF2 junction region, PCR amplification was also performed with a mixture of three forward primers, G2FB (5′-GGHCCMBMDTTYTACAGCAA-3′, 5′-GGHCCMBMDTTYTACAAGAA-3′, and 5′-GGHCCMBMDTTYTACARNAA-3′, correspond-

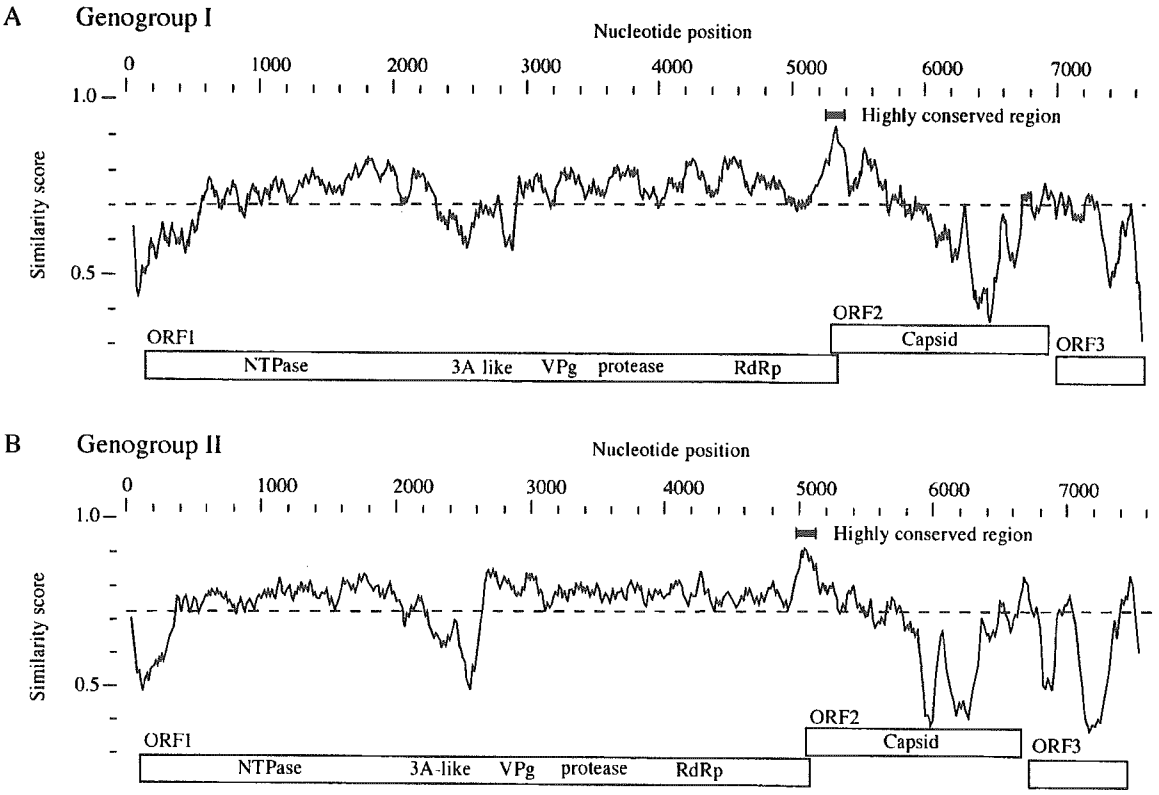

FIG. 1. Nucleotide sequences of full-length NLV genomes were analyzed with the PlotSimilarity program of Genetics Computer Group software. Similarity scores of a 150-nt sliding window were plotted. Four NLV GI strains (SzUGI, Norwalk/68, Southampton, and BS5) (A) and 10 NLV GII strains (U1, U3, U4, U16, U17, U18, U201, U25, Lordsdale, and Camberwell) (B) were compared. The locations of the ORFs are noted. Thick lines depict the most conserved regions. The average similarity score within each genogroup is represented as a dotted line.

ing to nt 4922 to 4941 in the Camberwell virus) and a reverse primer, G2SKR (21). The forward primers were designed by aligning the full-length NLV GI or GII sequences. RT was carried out as described previously (21). Ten microliters of cDNA was added to 40 μl of PCR mixture containing 5 μl of 10× Ex *Taq* buffer; 2.5 mM $MgCl_2$; 200 μM (each) dATP, dGTP, dTTP, and dCTP; 20 pmol of primers; and 2.5 U of Ex *Taq* DNA polymerase (Takara Shuzou, Kyoto, Japan). Conditions for PCR on the GeneAmp PCR system 9600 (Perkin-Elmer, Wellesley, Mass.) were as follows: initial denaturation at 95°C for 10 min; 40 amplification cycles with denaturation at 95°C for 30 s, annealing at 48°C for 30 s, and extension at 72°C for 2 min; and a final incubation at 72°C for 7 min. The 597-bp NLV GI PCR product corresponded to nt 5075 to 5671 in Norwalk/68, and the 468-bp NLV GII PCR product corresponded to nt 4922 to 5389 in Camberwell. The PCR product was cloned into TA-cloning vector pT7 Blue (Novagen, Madison, Wis.). The DNA sequence was determined from at least three clones with the BigDye terminator cycle sequence kit and ABI 377A sequencer (Applied Biosystems, Foster City, Calif.).

Conventional RT-PCR assays. A part of the RdRp gene was amplified with primers MR3 and MR4 for the first PCR (23) and with Yuri22F and Yuri22R (31) for the nested PCR. The capsid N-terminal/shell (N/S) domain was amplified with genogroup-specific primer pairs (21). RT-PCR was carried out as described previously (21). The PCR products were separated by electrophoresis in 3% agarose gels and visualized by ethidium bromide staining.

Real-time quantitative RT-PCR. To prevent carryover contamination by NLV cDNA and to reduce nonspecific amplification, viral RNA extracted with a QIAamp viral RNA kit was treated with DNase I before RT. Viral RNA (12.5 μl) was added to a reaction mixture (2.5 μl) containing DNase I buffer (150 mM Tris-HCl [pH 8.3], 225 mM KCl, 9 mM $MgCl_2$) and 1 U of RQ1 DNase (Promega Madison, Wis.). The reaction mixture was incubated at 37°C for 30 min to digest DNA and then at 75°C for 5 min to inactivate the enzyme. DNase I-treated RNA (15 μl) was added to 15 μl of another mixture containing 100 mM Tris-HCl (pH 8.3), 150 mM KCl, 6 mM $MgCl_2$, a 1 mM concentration of each deoxynucleoside triphosphate, 10 mM dithiothreitol, 75 pmol of random hexamers (pdN6; Amersham Pharmacia Biotech, Piscataway, N.J.), 30 U of RNasin (Promega), and 200 U of SuperScript II RNase H (−) reverse transcriptase (Gibco BRL, Gaithersburg, Md.). RT was performed at 42°C for 2 h, and the enzyme was inactivated at 70°C for 15 min. cDNA solutions were stored at −20°C.

The real-time quantitative RT-PCR was carried out in 50 μl of a reaction mixture containing 5 μl of cDNA, 25 μl of TaqMan Universal PCR Master Mix (Applied Biosystems) containing dUTP and uracyl *N*-glycosylase (UNG), a 400 nM concentration of each primer, and either 15 pmol of RING1(a)-TaqMan Probe (TP) and 5 pmol of RING1(b)-TP fluorogenic probes for NLV GI detection or 5 pmol of RING2-TP fluorogenic probe for NLV GII detection. PCR amplification was performed with an ABI Prism 7700 sequence detector (Applied Biosystems) under the following conditions: incubation at 50°C for 2 min to activate UNG, initial denaturation at 95°C for 10 min, and then 45 cycles of amplification with denaturation at 95°C for 15 s and annealing and extension at 56°C for 1 min. Amplification data were collected and analyzed with Sequence Detector software version 1.6 (Applied Biosystems).

In each operation, an NLV GI- or GII-specific standard curve was generated by a 10-fold serial dilution (10^7 to 10^1 copies) of purified NLV GI or GII cDNA plasmids. Plasmid standards containing PCR products of the ORF1-ORF2 junction were prepared with strains SzUG1 and U201 with primer sets G1FF-G1SKR and G2FB-G2SKR, respectively.

Genome sequences. The following partial and complete genome sequences were also used in this study: Norwalk/68, GenBank accession no. M87661; Southampton, L07418; Camberwell, AF145896; Lordsdale, X86557; BS5, AF093797; KY-89, L23828; Desert Shield, U04469; Chiba, AB042808; Melksham, X81879; Hawaii, U07611; Toronto, U02030; OTH-25, L23830; Arg320, AF190817; Bristol, X76716; Mexico, U22498; Queensarms, AJ313030; and OC98008, AF315812.

Nucleotide sequence accession numbers. The complete nucleotide sequences of the nine strains (19) were deposited in DDBJ with the following accession numbers: Saitama SzUG1 (SzUG1), AB039774; Saitama U1 (U1), AB039775;

TABLE 1. Detection of NLVs by using conventional RT-PCRs and real-time quantitative RT-PCR with 81 EM-positive stool specimens from 36 outbreaks of nonbacterial acute gastroenteritis

Outbreak			Stool code	Conventional RT-PCR		Real-time RT-PCR[b]
No.	Mo-yr	Place		For RdRp[a] (nested)	For capsid[b,c]	
1	Jan.-97	Restaurant	U1[d]	+	GII	GII
			U2[d]	+	GII	GII
2	Feb.-97	Food product	U3[d]	−	GII	GII
			U4[d]	−	GII	GII
3	Oct.-97	Nursery school	U5[d]	+	GII	GII
			U6[d]	+	GII	GII
			U27	+	GII	GII
			U28	+	GII	GII
4	Nov.-97	Nursing home	U7[d]	+	GII	GII
			U8[d]	+	GII	GII
5	Nov.-97	Food product	U9[d]	+	GII	GII
6	Dec.-97	Restaurant	U29	+	GII	GII
7	Dec.-97	Restaurant	U10[d]	−	GII	GII
			U11[d]	+	GII	GII
8	Dec.-97	Restaurant	U12[d]	+	GII	GII
			U13[d]	+	GII	GII
9	Jan.-98	Restaurant	U30	+	GII	GII
			U31	+	GII	GI + GII
10	Jan.-98	Restaurant	U32[d]	−	−	−
11	Jan.-98	Hotel	U201[d]	+	GII	GII
			U15[d]	+	GII	GII
12	Feb.-98	Dormitory	U16[d]	+	GII	GII
			U17[d]	+	GII	GII
13	May-98	School	U18[d]	+	GII	GII
			U19[d]	+	GII	GII
			U20[d]	+	GII	GII
			U21[d]	+	GII	GII
14	Dec.-98	Restaurant	U22[d]	+	GII	GII
			U23[d]	+	GII	GII
			U24[d]	+	GII	GII
15	Dec.-98	Restaurant	U25[d]	−	−	GII
			U26[d]	−	−	GII
16	Mar.-99	Hotel	KU4[d]	+	GI	GI
			KU6[d]	+	GI	GI
			KU7[d]	+	GI	GI
17	Apr.-99	Restaurant	KU8[d]	+	GI	GI
			KU9[d]	+	GII	GII
18	Apr.-99	Restaurant	KU10[d]	−	GI	GI
19	May-99	School	KU17[d]	−	GII	GII
20	May-99	School	KU24[d]	−	GI	GI
			KU25	−	GI	GI
21	Jun.-99	Hotel	KU34[d]	+	GII	GII
22	Jun.-99	Food product	KU44[d]	+	GII	GII

Continued on following page

TABLE 1—*Continued*

Outbreak			Stool code	Conventional RT-PCR		Real-time RT-PCR[c]
No.	Mo-yr	Place		For RdRp[a] (nested)	For capsid[b,a]	
23	Oct.-99	Restaurant	KU45	−	−	GII
24	Oct.-99	Nursery school	KU62[d]	+	−	GII
			KU63[d]	−	−	GII
			KU64[d]	−	−	GII
			KU66[d]	+	−	GII
25	Nov.-99	School	KU68[d]	+	GII	GII
26	Nov.-99	Restaurant[e]	KU80[d]	+	GI + GII	GI + GII
			KU82[d]	+	GI + GII	GI + GII
			KU83[d]	+	GI + GII	GI + GII
			KU84[d]	+	GII	GII
27	Dec.-99	School party	KU85[d]	−	GII	GII
			KU88[d]	+	GII	GII
			KU89[d]	+	−	GII
			KU90	+	GII	GII
			KU91	+	GII	GII
28	Dec.-99	School	KU93[d]	+	GII	GII
29	Dec.-99	Restaurant	KU98[d]	+	GII	GII
			KU99[d]	−		GII
			KU101[d]	+	GII	GII
30	Dec.-99	Restaurant	KU105[d]	+	GI + GII	GI + GII
			KU106	+	GI + GII	GI + GII
			KU109[d]	+	GI + GII	GI + GII
			KU111[d]	−	GI + GII	GI + GII
			KU112[d]	−	GI	GI
			KU115[d]	−	GI	GI
31	Jan.-00	Food product	KU5[d]	+	−	GII
32	Jan.-00	Family	KU16[d]	+	GII	GII
33	Jan.-00	Restaurant[e]	KU18[d]	+	GII	GII
			KU19[d]	+	GI + GII	GI + GII
			KU26[d]	+	GII	GII
			KU27[d]	−	GII	GII
34	Mar.-00	Restaurant	KU31[d]	+	−	GII
			KU32[d]	+	−	GII
35	Mar.-00	Restaurant[e]	KU35[d]	+	GII	GII
			KU36[d]	+	GI + GII	GI + GII
			KU37[d]	+	−	GII
36	Mar.-00	Hotel	KU49[d]	+	GII	GII
			KU53[d]	+	GII	GII
Total			81	62	67	80
Detection rate (%)				77	83	99

[a] +, positive; −, negative. Method described in reference 31.
[b] Method described in reference 21.
[c] GI, GI detected; GII, GII detected; −, negative.
[d] Used for sequence analysis.
[e] From shellfish-related outbreak.

Saitama U3 (U3), AB039776; Saitama U4 (U4), AB039777; Saitama U16 (U16), AB039778; Saitama U17 (U17), AB039779; Saitama U18 (U18), AB039781; Saitama U201 (U201), AB039782; and Saitama U25 (U25), AB039780. The nucleotide sequences of the ORF1-ORF2 junctions were submitted to DDBJ; the accession numbers were AB058511 to AB058529 and AB058534 to AB058598.

RESULTS

PlotSimilarity analysis. Our first goal was to identify a stable region suitable for designing new primers and probes for RT-PCR amplification. To identify the region with highest similar-

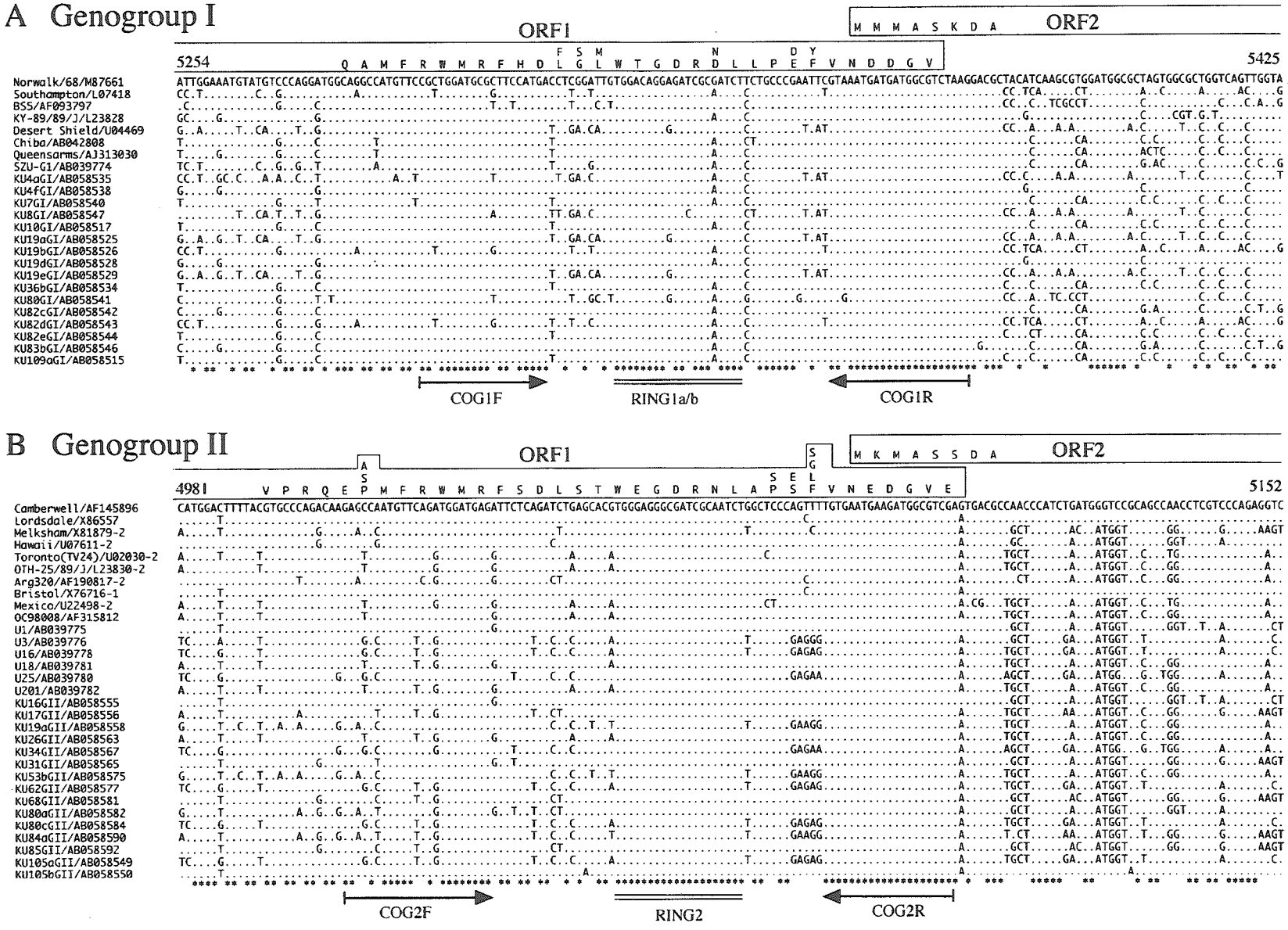
A Genogroup I
ORF1
ORF2
M M M A S K D A
5254
5425
Q A M F R W M R F H D L G L W T G D R D L L P E F V N D D G V
F S M
N
D Y
Norwalk/68/M87661
Southampton/L07418
BS5/AF093797
KY-89/89/J/L23828
Desert Shield/U04469
Chiba/AB042808
Queensarms/AJ313030
SZU-G1/AB039774
KU4aGI/AB058535
KU4fGI/AB058538
KU7GI/AB058540
KU8GI/AB058547
KU10GI/AB058517
KU19aGI/AB058525
KU19bGI/AB058526
KU19dGI/AB058528
KU19eGI/AB058529
KU36bGI/AB058534
KU80GI/AB058541
KU82cGI/AB058542
KU82dGI/AB058543
KU82eGI/AB058544
KU83bGI/AB058546
KU109aGI/AB058515
COG1F
RING1a/b
COG1R
B Genogroup II
ORF1
ORF2
M K M A S S D A
4981
5152
V P R Q E P M F R W M R F S D L S T W E G D R N L A P S F V N E D G V E
A
S
S G
S E L
Camberwell/AF145896
Lordsdale/X86557
Melksham/X81879-2
Hawaii/U07611-2
Toronto(TV24)/U02030-2
OTH-25/89/J/L23830-2
Arg320/AF190817-2
Bristol/X76716-1
Mexico/U22498-2
OC98008/AF315812
U1/AB039775
U3/AB039776
U16/AB039778
U18/AB039781
U25/AB039780
U201/AB039782
KU16GII/AB058555
KU17GII/AB058556
KU19aGII/AB058558
KU26GII/AB058563
KU34GII/AB058567
KU31GII/AB058565
KU53bGII/AB058575
KU62GII/AB058577
KU68GII/AB058581
KU80aGII/AB058582
KU80cGII/AB058584
KU84aGII/AB058590
KU85GII/AB058592
KU105aGII/AB058549
KU105bGII/AB058550
COG2F
RING2
COG2R

FIG. 2. Alignment of nucleotide sequences and partial predicted amino acid sequences of the ORF1-ORF2 junctions of NLV GI (A) and GII (B). The nucleotide sequences of NLV GI were aligned from nt 5254 to 5425 in Norwalk/68, and those of NLV GII were aligned from nt 4981 to 5152 in Camberwell. The strain name and accession number are shown beside its sequence; a lowercase letter in the strain name indicates a different clone from the same stool specimen. Some strains with identical sequence are omitted from the figure. The conserved amino acid sequences of NLV GI ORF1 are indicated above the sequences between nt 5279 and 5371 in Norwalk/68, and those of ORF2 are indicated between nt 5358 and 5381. The conserved amino acid sequences of NLV GII ORF1 are indicated above the nucleotide sequences between nt 4988 and 5101 in Camberwell, and those of ORF2 are indicated between nt 5085 and 5108. The asterisks below the alignment show consensus nucleotide sequences. Arrows and double lines show locations of newly designed primers and probes, respectively, used in this study.

ity, PlotSimilarity was used to analyze full-length NLV GI sequences, including those of SzUGI, Norwalk/68, Southampton, and BS5 (Fig. 1A), and NLV GII sequences, including those of U1, U3, U4, U16, U17, U18, U201, U25, Lordsdale, and Camberwell (Fig. 1B). The highest nucleotide similarity score was found in the ORF1-ORF2 junction region (the C-terminal RdRp to the N-terminal capsid) (19). We selected this region, corresponding to nt 5250 to 5530 in Norwalk/68 (GI) and to nt 4980 to 5260 in Camberwell (GII), as a promising candidate for the design of real-time quantitative RT-PCR primers and probes.

Nucleotide sequences of ORF1-ORF2 junction regions from 71 strains. To confirm that it is highly conserved within each genogroup, we sequenced the ORF1-ORF2 junction regions of NLVs isolated from 71 stool specimens (Table 1). We used RT-PCR and primer sets G1FF-G1SKR and G2FB-G2SKR to amplify the NLV GI and GII ORF1-ORF2 junction regions, respectively. All sequences of the ORF1-ORF2 junction region were determined from at least three clones. The cDNA sequences for 70 samples were submitted to DDBJ (see Materials and Methods). Only one stool specimen, stool code U32, was not amplified by this RT-PCR.

Multiple alignment of the ORF1-ORF2 junction region was performed on each genogroup and with available sequences in the database (Fig. 2). Some stool specimens appeared to contain both NLV GI and GII sequences (e.g., KU80 and KU19) (Fig. 2). Four stool specimens (i.e., KU4, KU80, KU105, and KU19) contained two or more NLVs with sequence variants belonging to the same genogroup (Fig. 2). Multiple alignment of the ORF1-ORF2 junction region revealed that the most highly conserved nucleotide sequences were nt 5279 to 5381 (102 bases) with respect to Norwalk/68 virus (M87661) among NLV GI and nt 4988 to 5108 (120 bases) with respect to Camberwell virus (AF145896) among NLV GII. In this region, the nucleotide identities within the genogroups were 88 to 100% and 86 to 100%, respectively. Interestingly, 20 nt (nt 5357 to 5376 in Norwalk/68) or 21 nt (nt 5080 to 5100 in Camberwell) overlapped by ORF1 and ORF2 exhibited a perfect match within NLV GI or GII, respectively.

Development of real-time quantitative RT-PCR. We designed genogroup-specific primer sets and fluorescent probes in the NLV ORF1-ORF2 junction region for use in real-time quantitative RT-PCR. The primer pair COG1F-COG1R and a mixture of fluorescent probes, RING1(a)-TP and RING1(b)-TP, were used to detect NLV GI. The primer pair COG2F-COG2R and the fluorescent probe RING2-TP were used to detect GII NLVs. The locations of the primers and fluorescent probes are illustrated in Fig. 2, and the nucleotide sequences are shown in Table 2.

To determine the dynamic range of the real-time quantitative RT-PCR, we generated standard curves with 10-fold serial dilutions of NLV GI and GII standard plasmids (from 10^7 to 10^1 copies) (Fig. 3). The amplification curves shifted to the right as the initial amount of the plasmid was reduced (Fig. 3A and B). We constructed standard curves of the threshold cycle (Ct) of the NLV GI and GII standard plasmid against the amount of plasmid (Fig. 3C and D). The correlation between the Ct and the amount of target template was good between 10^7 and 10^1 copies. Cross-reactivity between GI and GII was not observed when the plasmid standards were used.

TABLE 2. Primer and probe oligonucleotides used for real-time quantitative RT-PCR

Genogroup	Primer or probe	Sequence (5′ → 3′)[a]	Polarity[b]	Location
GI	Primer COG1F	CGYTGGATGCGNTTYCATGA	+	5291[e]
	Primer COG1R	CTTAGACGCCATCATCATTYAC	−	5375[e]
	Probe[c] RING1(a)-TP	FAM-AGATYGCGATCYCCTGTCCA-TAMRA[d]	−	5340[e]
	RING1(b)-TP	FAM-AGATCGCGGTCTCCTGTCCA-TAMRA	−	5340[e]
GII	Primer COG2F	CARGARBCNATGTTYAGRTGGATGAG	+	5003[f]
	Primer COG2R	TCGACGCCATCTTCATTCACA	−	5100[f]
	Probe RING2-TP	FAM-TGGGAGGGCGATCGCAATCT-TAMRA	+	5048[f]

[a] Mixed bases in degenerate primers and probes are as follows: Y, C or T; R, A or G; B, not A; N, any.
[b] +, virus sense; −, anti-virus sense.
[c] Mixed probes are used for the GI NLVs.
[d] 6-Carboxyfluorescein (FAM) as the reporter dye is coupled in the 5′ end of the oligonucleotide, and 6-carboxy-tetramethylrhodamine (TAMRA) as the quencher dye is coupled in the 3′ end of the oligonucleotide.
[e] Corresponding nucleotide position of Norwalk/68 virus (accession no. M87661) of the 5′ end.
[f] Corresponding nucleotide position of Camberwell virus (accession no. AF145896) of the 5′ end.

Quantitative detection of NLV RNA. Real-time quantitative RT-PCR was used to detect NLV RNAs from 81 EM-positive stool specimens for evaluation (Table 1). NLV RNA was detected in 80 (99%) of 81 stool specimens, whereas conventional RT-PCR detected NLV in 62 of 81 stool specimens (77%) for the RdRp and in 67 of 81 (83%) for the capsid N/S region (Table 1). All three RT-PCR methods failed to detect NLV RNA from stool code U32.

Of 80 real-time quantitative RT-PCR-positive and EM-positive stool specimens, nine contained NLV GI viruses and 61 contained NLV GII viruses. Interestingly, 10 stool specimens (U31, KU80, KU82, KU83, KU105, KU106, KU109, KU111,

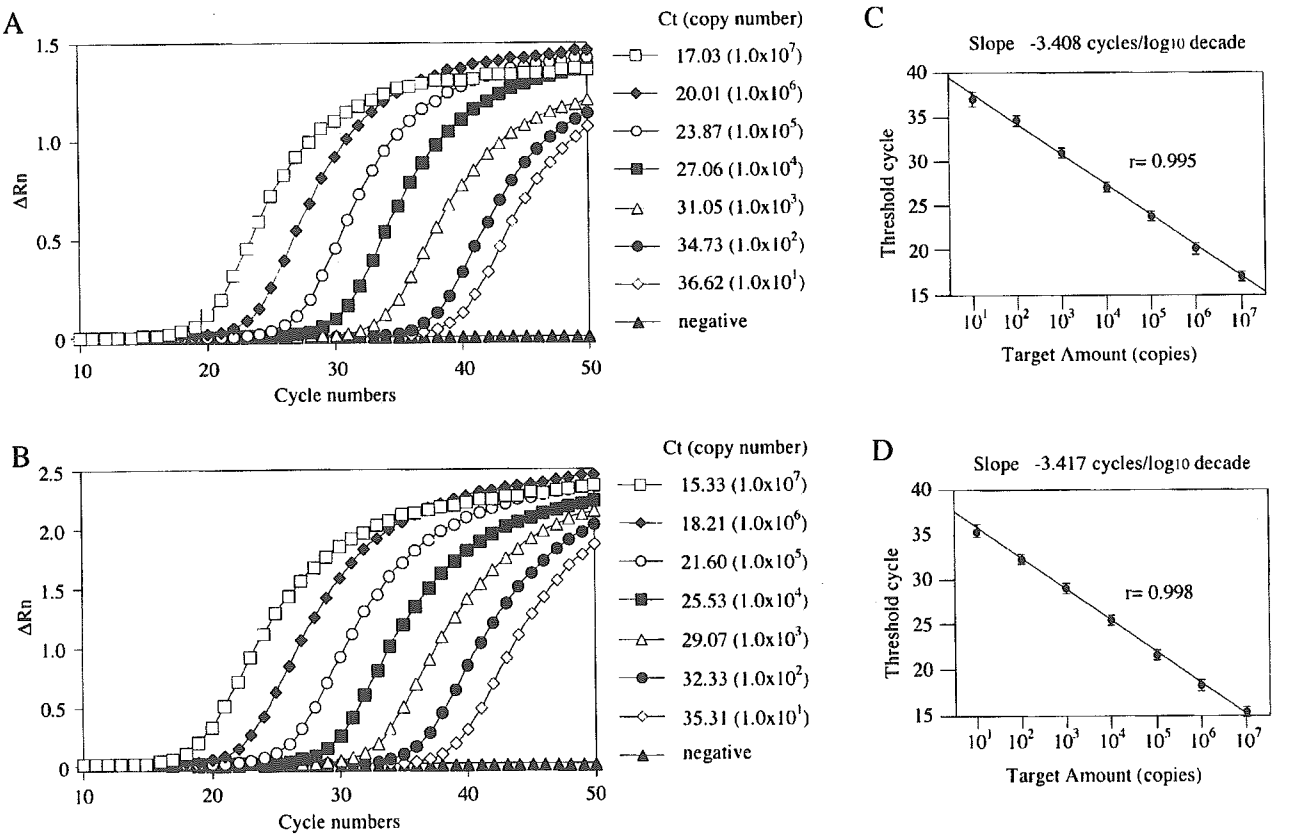

FIG. 3. Real-time RT-PCR quantification of NLV GI and GII standard plasmids. (A and B) Amplification plots of fluorescence intensities (ΔRn) versus the PCR cycle numbers are displayed for serial 10-fold dilutions of standard plasmids (10^7 to 10^1 copy equivalents per reaction) for NLV GI (A) and GII (B). Each plot corresponds to a particular input target quantity marked by a corresponding symbol. Results are the average of those from three reactions. (C and D) Relationship of known numbers of NLV GI (C) and GII (D) standard plasmids to the threshold cycle (Ct). The Ct is directly proportional to the log of the input copy equivalents, as demonstrated by the standard curve. Results are the average of those from three reactions, and error bars indicate standard deviations.